

AD-774 385

**A SHOCK TUBE STUDY OF THE IGNITION OF
MIXTURES OF N₂O, CO, AND N₂**

Robert E. Case

**Air Force Institute of Technology
Wright-Patterson Air Force Base, Ohio**

December 1973

DISTRIBUTED BY:

NTIS

**National Technical Information Service
U. S. DEPARTMENT OF COMMERCE
5285 Port Royal Road, Springfield Va. 22151**

UNCLASSIFIED

Security Classification

AD 774385

DOCUMENT CONTROL DATA - R & D

(Security classification of title, body of abstract and indexing annotation must be entered when the overall report is classified)

1. ORIGINATING ACTIVITY (Corporate author)

Air Force Institute of Technology (AFIT-EN)
Wright-Patterson Air Force Base, Ohio 45433

2a. REPORT SECURITY CLASSIFICATION

Unclassified

2b. GROUP

3. REPORT TITLE

A Shock Tube Study of Ignition of Mixtures of N_2O , CO, and N_2

4. DESCRIPTIVE NOTES (Type of report and inclusive dates)

AFIT Thesis

5. AUTHOR(S) (First name, middle initial, last name)

Robert E. Case
Captain USAF

6. REPORT DATE

December 1973

7a. TOTAL NO. OF PAGES

52 44

7b. NO. OF REFS

14

8a. CONTRACT OR GRANT NO.

8b. ORIGINATOR'S REPORT NUMBER(S)

a. PROJECT NO.

N/A

GA/ME/73A-1

9b. OTHER REPORT NO(S) (Any other numbers that may be assigned this report)

10. DISTRIBUTION STATEMENT

Approved for public release; distribution unlimited.

Approved for public release; IAW AFR 190-17

11. SPONSORING MILITARY ACTIVITY

JERRY C. HIX, Captain, USAF
Director of InformationAir Force Weapons Laboratory
Kirtland AFB, New Mexico

12. ABSTRACT

A shock tube was employed to determine ignition limit curves for three gas mixtures of N_2O , CO, and N_2 . The gas mixtures were ignited by the temperature rise behind the reflected shock wave. A 2-inch inner diameter constant area shock tube using a helium driver gas was used to ignite gas mixtures of 60% N_2 , 20% CO, 20% N_2O ; 70% N_2 , 15% CO, 15% N_2O ; and 80% N_2 , 10% CO, 10% N_2O . Limited ignition delay time was also obtained for all three mixtures.

Reproduced by
NATIONAL TECHNICAL
INFORMATION SERVICE
U S Department of Commerce
Springfield VA 22131

14.

KEY WORDS

LINK A

LINK B

LINK C

ROLE

WT

ROLE

WT

ROLE

WT

Ignition limit curve

Shock tube technique

Nitrous oxide and carbon monoxide ignition

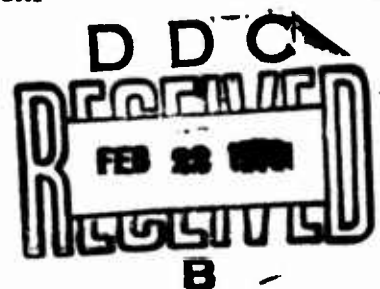
Ignition delay time

A SHOCK TUBE STUDY OF THE IGNITION OF
MIXTURES OF N_2O , CO, AND N_2

THESIS

GA/ME/73A-1

Robert E. Case
Captain USAF



Approved for public release; distribution unlimited.

A SHOCK TUBE STUDY OF THE IGNITION OF
MIXTURES OF N_2O , CO , AND N_2

THESIS

Presented to the Faculty of the School of Engineering
of the Air Force Institute of Technology

Air University

in Partial Fulfillment of the
Requirements for the Degree of

Master of Science

by

Robert E. Case, B.S.

Captain USAF

Graduate Astronautical Engineering

December 1973

Approved for public release; distribution unlimited.

ic

Preface

This thesis is an in-house project conducted under the guidance of the Ramjet Components Branch, Ramjet Engine Division of the Air Force Aero Propulsion Laboratory, Research and Technology Division, Wright-Patterson Air Force Base, Ohio. This study was conducted under Task 3012-1401 of Project 3012, "Ramjet Technology."

The author wishes to express sincere appreciation to Dr. William C. Elrod for serving as overall thesis advisor and Dr. Paul J. Ortwerth, formerly of the Aero Propulsion Laboratory, for serving as research advisor. Their interest and advice were vital to the successful completion of this study. Appreciation is also extended to Dr. Ernest A. Dorko and Maj. Robert F. Bestgen for their interest and advice as members of the thesis advisory committee.

Special acknowledgment is made to several members of the Aero Propulsion Laboratory. Appreciation is expressed to Dr. Roger R. Craig for his expert advice concerning the entire operation of the shock tube. Also included are the laboratory technicians, Messrs. R. Schelenz, R. Allen, H. Day, and T. Williams for their exceptional assistance during the experimental phase of the study.

The author expresses heartfelt appreciation for the support and patience of his wife, [REDACTED] during the preparation of this report.

Robert E. Case

Contents

	Page
Preface	ii
List of Figures	v
List of Tables	vii
List of Symbols and Abbreviations	viii
Abstract	x
I. Introduction	1
Background	1
Purpose and Scope	2
II. Shock Tube Description	3
III. Test Apparatus and Procedure	5
Facility	5
Shock Tube	5
Test Section	5
Instrumentation and Support Equipment	6
Burst Diaphragms	6
Test Procedure	9
Single Diaphragm Mode	9
Double Diaphragm Mode	9
Test Gas Mixtures	11
IV. Data Reduction	12
Incident Shock Wave Mach Number, M	12
Reflected Shock Temperature, T_5	14
Reflected Shock Pressure, P_5	18
Ignition Delay Time, τ_{ig}	23
V. Discussion of Results	25
Flame Spectrum Analysis	25
Ignition Limit	27
Ignition Delay Time	31
VI. Conclusions and Recommendations	36
Conclusions	36
Recommendations	36

	Page
Bibliography	38
Appendix A: Test Data	40
Appendix B: Reflected Shock Temperature and Pressure Ratios . .	49
Vita	52

List of Figures

Figure		Page
1	Test Instrumentation	7
2	Schematic of Test Instrumentation and Support Equipment	8
3	Reflected Shock Temperature Ratio for 60% N ₂ , 20% CO, 20% N ₂ O	15
4	Reflected Shock Temperature Ratio for 70% N ₂ , 15% CO, 15% N ₂ O	16
5	Reflected Shock Temperature Ratio for 80% N ₂ , 10% CO, 10% N ₂ O	17
6	Reflected Shock Pressure Ratio for 60-20-20	19
7	Reflected Shock Wave Pressure Ratio for 70-15-15	20
8	Reflected Shock Wave Pressure Ratio for 80-10-10	21
9	Diagram of Oscilloscope Trace for Test Run Without Ignition	22
10	Photograph of Oscilloscope Trace for a Test Run Without Ignition	22
11	Photographs of Two Test Runs with Different Ignition Delay Times	24
12	Modified Fisher Burner for Flame Spectrum Analysis	26
13	Ignition Limit Curve for 60-20-20 Mixture Ignited Behind a Reflected Shock Wave	28
14	Ignition Limit Curve for 70-15-15 Mixture Ignited Behind a Reflected Shock Wave	29
15	Ignition Limit Curve for 80-10-10 Mixture Ignited Behind a Reflected Shock Wave	30
16	Ignition Delay Time for 60-20-20 Mixture Ignited Behind a Reflected Shock Wave	32

Figure		Page
17	Ignition Delay Time for 70-15-15 Mixture Ignited Behind a Reflected Shock Wave	33
18	Ignition Delay Time for 80-10-10 Mixture Ignited Behind a Reflected Shock Wave	34

List of Tables

Table		Page
I	Ignition limit data for 60% N ₂ , 20% CO, 20% N ₂ O (Fig 13)	40
II	Ignition limit data for 70% N ₂ , 15% CO, 15% N ₂ O (Fig 14)	42
III	Ignition limit data for 80% N ₂ , 10% CO, 10% N ₂ O (Fig 15)	44
IV	Ignition delay data for 60% N ₂ , 20% CO, 20% N ₂ O (Fig 16)	46
V	Ignition delay data for 70% N ₂ , 15% CO, 15% N ₂ O (Fig 17)	47
VI	Ignition delay data for 80% N ₂ , 10% CO, 10% N ₂ O (Fig 18)	48
VII	T ₅ /T ₁ and P ₅ /P ₁ versus M values for the 60% N ₂ , 20% CO, 20% N ₂ O test gas mixture with helium driver (Figs 3 and 6)	49
VIII	T ₅ /T ₁ and P ₅ /P ₁ versus M values for the 70% N ₂ , 15% CO, 15% N ₂ O test gas mixture with helium driver (Figs 4 and 7)	50
IX	T ₅ /T ₁ and P ₅ /P ₁ versus M values for the 80% N ₂ , 10% CO, 10% N ₂ O test gas mixture with helium driver (Figs 5 and 8)	51

List of Symbols and Abbreviations

<u>Symbol</u>	<u>Meaning</u>
a	speed of sound = $\sqrt{\gamma RT}$, ft/sec
\AA	angstrom
g_c	universal gravitational constant = 32.174 lbm ft/lbf sec ²
M	shock wave Mach number
P	pressure, psi or atm
PPM	parts per million
R	gas constant, ft ² /sec ² °R
τ_{ig}	ignition delay time, msec
T	temperature, °R or °K
V.P.F.	voltage-pressure factor, the combined scale factor for the Kistler pressure transducer and charge amplifier, mv/psi
V.T.S.	variable time setting, sweep rate for oscilloscope, msec/cm
V.V.S.	variable voltage setting for oscilloscope, mv/cm
W	incident shock wave speed, ft/sec
Δh	vertical distance measured on photograph of oscilloscope trace corresponding to $P_5 - P_1$, cm
Δs	distance between the two Kistler pressure transducers in the test section, 49.25 in
Δt	time interval measured by electronic counter for incident shock to traverse distance Δs , msec
Δw	horizontal distance measured on photograph of oscilloscope trace corresponding to ignition delay time, cm
γ	specific heat ratio
1	subscript denoting the state conditions in the driven section before diaphragm rupture
5	subscript denoting the state conditions in the driven section behind the reflected shock wave

<u>Abbreviation</u>	<u>Meaning</u>
atm	atmospheres pressure
He/air	helium-air system, where helium is the driver gas and air is the driven gas
He/test gas	helium-test gas system, where helium is the driver gas and a test gas mixture is the driven gas
msec	millisec
μsec	microseconds

Abstract

→ A shock tube was employed to determine the ignition limit of three mixtures of N_2O , CO , and N_2 . The ignition limit curve, which separates the ignition and no-ignition zones, is an experimentally determined curve plotted on temperature-pressure coordinates. The test gas mixtures of N_2O , CO , N_2 were ignited by the temperature rise behind the reflected shock wave for pressures in the range of 5 to 65 atmospheres. A 2-inch inside diameter constant area shock tube employing a helium driver was used to generate this reflected shock wave.

The results show that the ignition temperature for the 60% N_2O , 20% CO , 20% N_2 mixture decreases linearly as the pressure increases from about 1120°K at 5 atm to about 1000°K at 65 atm. The ignition temperature for the 70-15-15 mixture decreases as the pressure increases from about 1145°K at 5 atm to about 1060°K at 65 atm. This decrease is also linear but exhibits a lesser rate of decrease than the 60-20-20 mixture. The ignition temperature of the 80-10-10 mixture appears to decrease slightly and linearly from about 1210°K at 5 atm to about 1200°K at 65 atm. Hence, the ignition temperature is dependent on the amount of CO and N_2O present and on pressure (in the range tested).

In addition to ignition temperature data, limited results were obtained on ignition delay time for each of the three gas mixtures. ← A definite pressure-temperature correlation exists for each gas mixture. Increasing the temperature at a given pressure or increasing the pressure at a given temperature has the effect of reducing ignition delay time. Also, at a given pressure, ignition delay time decreases as the amount of N_2O and CO is increased.

A SHOCK TUBE STUDY OF THE IGNITION OF
MIXTURES OF N_2O , CO , AND N_2

I. Introduction

The development of the gas dynamic laser (GDL) has focused attention on the many problems involved with supersonic gas flow in the optical cavity of a laser. In particular, the CO_2 gas dynamic laser is of current interest and the search for better fuel-oxidizer combinations to produce CO_2 and N_2 is being intensified. One of the fuel-oxidizer combinations that is being considered is that of nitrous oxide (N_2O) and carbon monoxide (CO), diluted with nitrogen (N_2). The study described herein is a direct result of the attempt to apply the N_2O , CO reaction to the gas dynamic laser.

Background

Very few ignition and combustion studies of N_2O and CO have been reported. The flame temperature and flame velocity of gaseous mixtures with N_2O as the oxidant were analyzed by Van Wouterghem and Van Tiggelen in 1955 (Ref 1). Their tests were conducted with the combustion taking place at atmospheric pressure and with varying percentages of nitrogen (0% - 40%) in the total gas mixtures. Lin and Bauer performed an exhaustive study of the nitrous oxide and carbon monoxide reaction with argon being the inactive third body (Ref 2). However, their study was primarily to determine the kinetics of the reaction and not ignition

temperature data and ignition delay data. Lin and Bauer performed tests using a single-pulse shock tube and produced useful information concerning the use of a shock tube in studying gaseous reactions. They concluded that the bimolecular reaction:



was the predominant reaction for temperatures below 1640°K. Soloukhin performed a shock tube study of the N_2O , CO reaction at high temperatures (1600-3200°K) with argon as the inert third body (Ref 3). He confirmed Lin and Bauer's conclusion that the N_2O , CO proceeds via the radical-chain method at high temperatures and not the simple bimolecular reaction, which is predominant at lower temperatures (<1600°K).

Purpose and Scope

Until now, no study has been made on the ignition of N_2O , CO, and N_2 in the range of mixture ratios of 60% N_2 , 20% N_2O , 20% CO through 80% N_2 , 10% N_2O , 10% CO. The purpose of this study was to establish the ignition limit curve and ignition delay data for three mixtures of N_2O , CO, and N_2 for the pressure range of 5 to 65 atmospheres. This study determines the effect of pressure, temperature, and mixture ratios on the ignition of N_2O and CO by using a constant area shock tube to generate controlled temperature and pressures behind a reflected shock wave in the test gas mixture.

II. Shock Tube Description

The theory of shock tube operation is well understood and described in detail in the literature (Refs 4,5,6,7,8,9). However, a brief description is presented here as a ready reference for the reader and for understanding the method of igniting the test samples of gas mixtures.

The shock tube is a device in which a plane shock wave is generated by bursting a diaphragm which separates a gas at high pressure from one at lower pressure (Refs 4,5). A high pressure gas is contained in the driver section, separated by a diaphragm from the lower pressure gas in the driven section. When the diaphragm is ruptured, a shock wave travels into the driven section and heats the driven gas. A rarefaction fan propagates into the driver section at the same time. The contact surface (interface between the driver and driven gases) moves into the driven section at the same velocity as the gas behind the incident shock wave. The incident shock wave reflects from the end plate and returns, passing again through the driven gas until it interacts with the contact surface (Ref 10).

The shock tube in the reflected shock mode provides a method of generating a rectangular temperature pulse which is very suitable for high temperature ignition studies. The temperature of the gas behind the reflected shock wave increases rapidly to a high value. Temperatures up to 3000°K are easily achieved with moderate driver pressures (500 psia). There is a temperature increase across the incident shock wave, but this change is small relative to the reflected shock

temperature increase (Ref 10). The gas behind the reflected shock wave is at rest relative to the shock tube and allows direct observation of the reaction taking place in the high temperature (Ref 4). There is also no mixing of the driver gas with the driven gas, and thus the driver gas does not influence the reaction in any manner (Ref 2).

III. Test Apparatus and Procedure

Facility

The test apparatus employed in this study included a constant area shock tube with a test section mounted on the driven end along with instrumentation and support equipment. This facility is located in the Aero Propulsion Laboratory at Wright-Patterson Air Force Base, Ohio.

Shock Tube. The shock tube is constructed of type 321 stainless steel tubing with an overall length of 50 feet. It consists of ten 5-foot segments with a 2-inch inner and 4-inch outer diameter. For this study, the driver section was 25 feet and the driven section was 15 feet. This length-to-diameter ratio of 90 for the driven section is within the range of 50 to 100 which is recommended for this type investigation (Refs 4,5). Helium was the driver gas and the various gas mixtures of N_2O , CO, and N_2 were the driven gases.

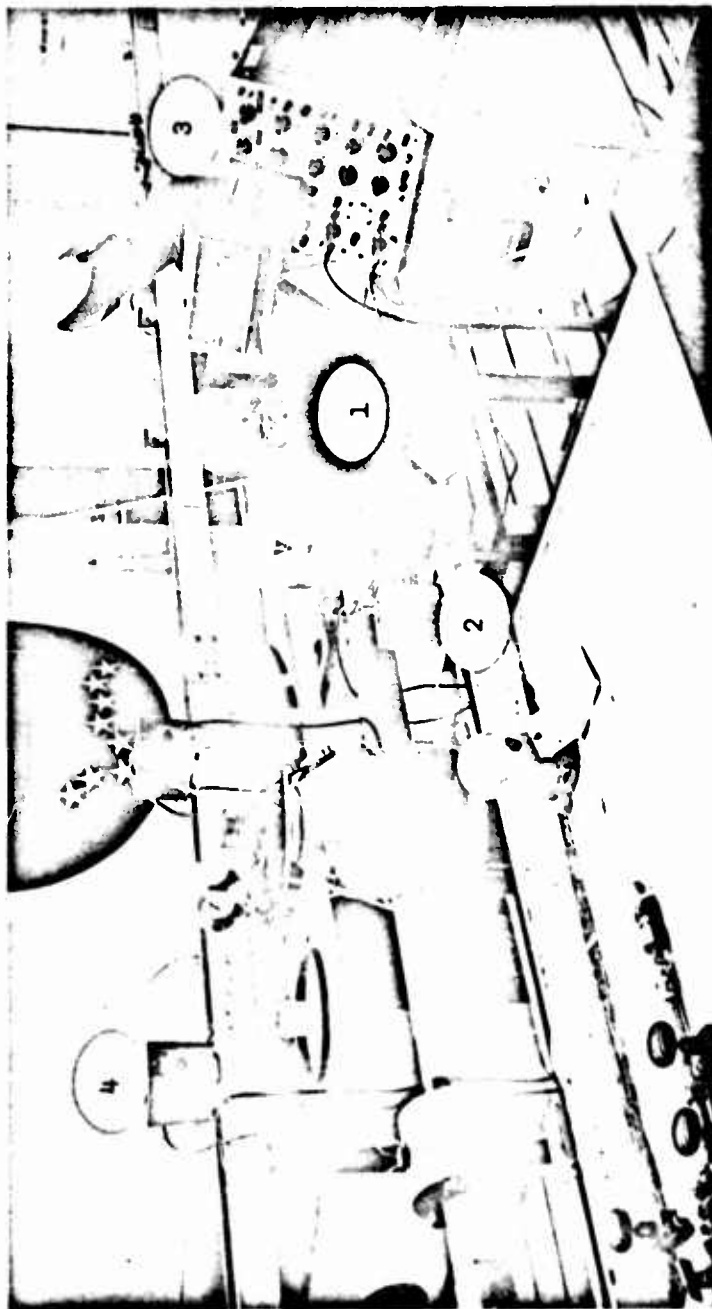
Test Section. The last 5-foot segment of the driven section was used as the test section. One 1/2-inch diameter quartz window was located 6 inches from the end plate to monitor the N_2O , CO ignition luminosity. Two quartz crystal pressure transducers were located in the test section. One was mounted opposite the middle of the window to measure the pressure of the combusting mixture, while another transducer was located at the beginning of the test section. The signals from these two transducers provided the means of measuring the incident shock wave speed.

Instrumentation and Support Equipment

In addition to the instrumentation necessary to record the test data (Fig 1), certain items of support equipment were necessary to operate the shock tube. A schematic drawing of the shock tube, instrumentation and support equipment is presented in Fig 2. These items are listed below:

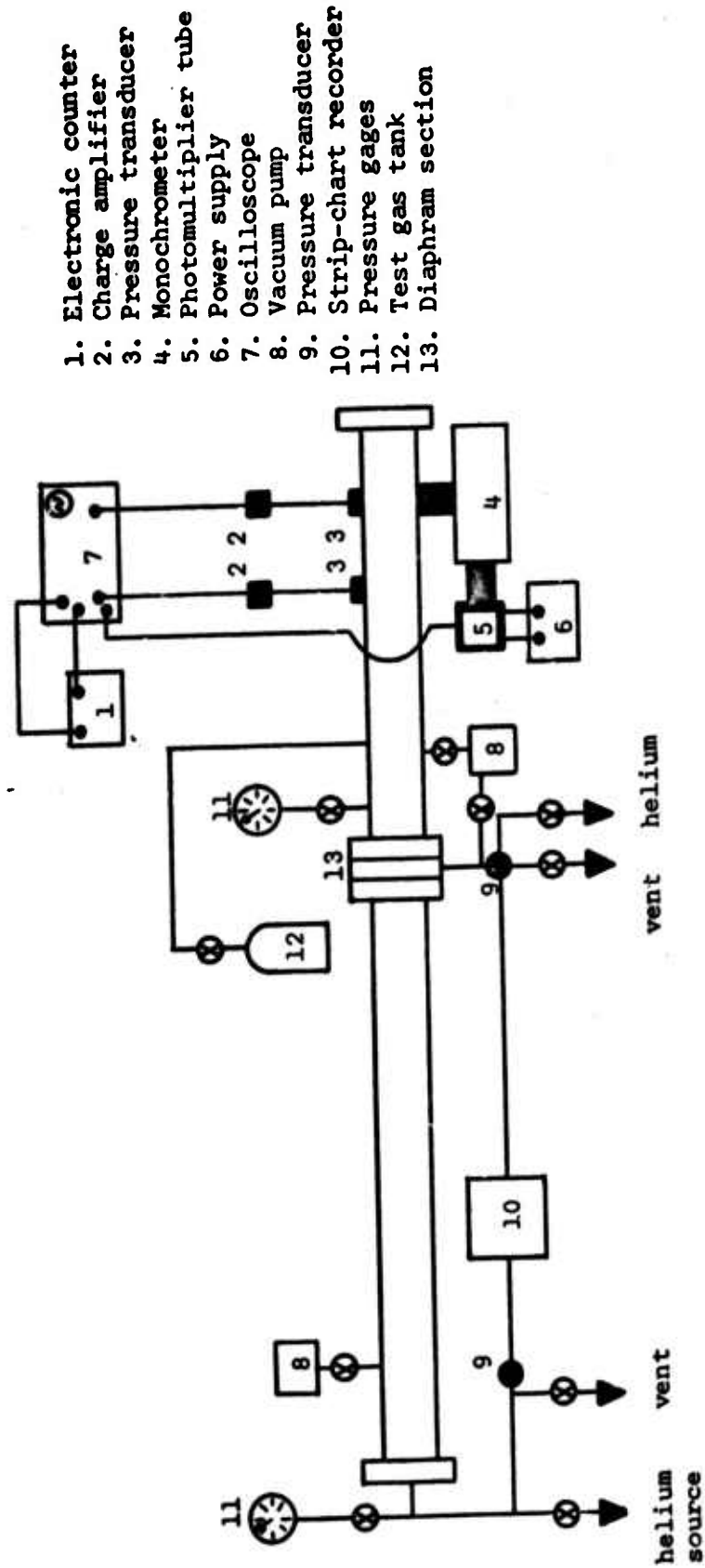
1. Electronic Counter, Hewlett and Packard, Model 523CR
2. Charge Amplifier, Kistler 566
3. Quartz Pressure Transducers, Kistler 601H and 603A
4. Diffraction Grating Monochrometer, Edmund Scientific Co.
5. Photomultiplier Tube, Dumont 6292
6. Power Supply, Litton Industries, Model 1043
7. Oscilloscope, Tektronic 535-A
8. High Vacuum Pumps, Kinney KC-8
9. Pressure Transducers, Statham Laboratories
10. Chart-drive Recorder, Brown Electronik
11. Absolute Pressure Gages, Wallace and Tiernan, Model FA-160
12. Test Gas Mixture Tank
13. Camera, Tektronic Series 125

Burst Diaphragms. Metal and plastic burst diaphragms were employed. Single diaphragms of various thickness plastic mylar were ruptured at their natural burst pressures. For higher burst pressures, several layers of plastic diaphragms were ruptured simultaneously. Stainless steel and aluminum diaphragms (scribed with crosswise score marks) were also used at higher pressures.



- 1. Monochromator
- 2. Photomultiplier tube
- 3. Oscilloscope and camera
- 4. Charge amplifiers

Figure 1. Test Instrumentation



Test Procedure

Before each test run the driven section was cleaned thoroughly with a high pressure airhose and a soft cloth which was pulled through the tube. The end plate was secured and a new diaphragm inserted into the diaphragm section. One of two possible operating modes of the diaphragm section was selected, depending on the pressures desired for a particular run. If the natural burst pressure of a diaphragm was near the value required to produce the desired ignition conditions in the test section, the single diaphragm mode was used; otherwise, the double diaphragm mode was used.

Single Diaphragm Mode. A diaphragm of known burst pressure (based on trial runs) was inserted into the diaphragm section in the single diaphragm mode (SD). The driver section was evacuated to about 2 mm Hg pressure. The driven section was evacuated to about 0.5 mm Hg and then filled with the desired test gas mixture of N_2O , CO, and N_2 to a selected pressure. The electronic equipment was then set and the camera shutter opened. All electrical lights in the laboratory were extinguished to eliminate extraneous light from entering the monochrometer. The driver section was then filled with helium until rupture of the diaphragm.

Double Diaphragm Mode. In the double diaphragm (DD) mode, two diaphragms, separated by one inch, were used. This innerspace between the two positions is called the DD section. After the two diaphragms were inserted, the driver section was evacuated to about 2 mm Hg pressure. The driven section and the DD section were evacuated to about 0.5 mm Hg. The driven section was filled with the desired test

gas mixture of N_2O , CO , and N_2 to a selected pressure. The driver and LD sections were filled simultaneously with helium to approximately one-half the final desired driver pressure. The DD section helium feed valve was then closed and the driver section allowed to continue filling until the final desired pressure was achieved. The electronic equipment was then set and the camera shutter opened. All electrical lights in the laboratory were extinguished to eliminate extraneous light from entering the monochrometer. The DD section was suddenly vented, rupturing both diaphragms.

With the time increment between the two Kistler pressure transducers measured by the electronic counter, the incident shock Mach number (M) was calculated. Then the temperature (T_5) behind the reflected shock wave was determined by using a theoretical curve for T_5/T_1 versus M for an equilibrium test gas mixture. From the oscilloscope pressure trace, the pressure (P_5) behind the reflected shock wave was computed. This experimental P_5 served as a check on the P_5 determined by using a theoretical curve for P_5/P_1 versus M for an equilibrium test gas mixture. More information on the theoretical analysis is in section IV, "Reflected Shock Temperature, T_5 ." Evidence of ignition was determined by the photomultiplier trace on the oscilloscope photograph. Information on ignition delay time was also determined from the pressure and photomultiplier traces. More detailed data reduction methods follow in section IV.

Test Gas Mixtures

Commercial "K" bottles of nitrous oxide, carbon monoxide and nitrogen were obtained from the Matheson Company. The listed purity of these gases were 98.0% for the N_2O , 99.5% for the CO, and 99.9% for the N_2 . No further purification was attempted. The impurities listed by Matheson Company were:

for the N_2	Ar . . . 400 PPM
	O_2 . . . 100 PPM
	CO_2 . . . 10 PPM
for the CO	N_2 . . . 1500 PPM
	O_2 . . . 600 PPM
	CO_2 . . . 50 PPM
for the N_2O	air. . . principal

The mixtures of N_2O and CO in N_2 were prepared in clean, empty air "K" bottles. These bottles were evacuated to lower than 0.10 mm Hg and then the N_2O , CO, and N_2 were fed into the bottle one at a time. A total mixture pressure of 100 psia was mixed using the partial pressures of the constituents necessary to achieve the desired gas ratios. The ratios used were 60% N_2O , 20% CO, 20% N_2 ; 70% N_2O , 15% CO, 15% N_2 ; and 80% N_2O , 10% CO, 10% N_2 . A heat lamp was then placed next to the base of the test gas "K" bottle, and the constituents allowed to mix convectively for at least 24 hours. The mixture was then allowed to mix by diffusion for at least another 24 hours before use in the shock tube.

IV. Data Reduction

Experimental data necessary to establish the ignition limit curves and information on ignition delay time were obtained for pressures ranging from 5 to 65 atm. Test gas mixtures of N_2O , CO , and N_2 were ignited by the reflected shock wave. The initial conditions in the driver and driven sections were based on a theoretical analysis of a He/test gas mixture shock tube system. This analysis made allowance for variable specific heats and formed the basis for reducing the experimental data.

Incident Shock Wave Mach Number, M

The Mach number of the incident shock wave was determined from the relationship

$$M = \frac{W}{a_1} \quad (1)$$

where W is the incident shock velocity, and a_1 is the speed of sound in test gas in the driven section. Since

$$W = \frac{\Delta s}{\Delta t} \quad (2)$$

and

$$a_1 = \sqrt{\gamma_1 g_c R_1 T_1} \quad (3)$$

where Δs is the distance between the two pressure transducers (49.25 in) and Δt is the time to traverse distance Δs (counter reading in μsec), and where

γ_1 = specific heat ratio of each test gas in driven section

= 1.373 for 60-20-20 mixture

= 1.379 for 70-15-15 mixture

= 1.386 for 80-10-10 mixture

R_1 = gas constant for each test gas in driven section

= 49.499 ft lbf/lbm °R for 60-20-20 mixture

= 50.800 ft lbf/lbm °R for 70-15-15 mixture

= 52.170 ft lbf/lbm °R for 80-10-10 mixture

T_1 = initial temperature of gas mixture in driven section,
°R

Since T_1 never varied more than 5°F, γ_1 was assumed to be constant for each mixture. After combining equations (1), (2), and (3) using appropriate conversion factors, the incident shock wave Mach number relationship is

$$M = \frac{\Delta s(10^6)}{12\Delta t \sqrt{\gamma_1 g_c R_1 T_1}} \quad (4)$$

With $T_1 = 540^\circ\text{R}$ and the γ_1 and R_1 corresponding to each test gas mixture, the incident shock wave Mach number relationship becomes

$$M = \frac{3.777(10^3)}{\Delta t} \quad (5)$$

$$M = \frac{3.719(10^3)}{\Delta t} \quad (6)$$

$$M = \frac{3.661(10^3)}{\Delta t} \quad (7)$$

for the 60-20-20, 70-15-15, and 80-10-10 mixtures, respectively, and where Δt = the counter reading in μsec .

Reflected Shock Temperature, T_5

The reflected shock temperature was determined from the incident Mach number and initial conditions. Because of the short duration of a normal run, typically 0.5 to 2 milliseconds, a simple, accurate measurement of T_5 was virtually impossible. However, a theoretical value of T_5 can be obtained from M and the initial conditions, as they are related through the basic fluid dynamic equations of continuity, energy, and momentum. In the general case of a gas with variable specific heats, an iterative procedure is required to obtain the reflected shock state conditions (temperature and pressure). This procedure has been carried out by Craig (Ref 11) for a He/Air System. His computer program was modified by replacing his enthalpy expression (for air) with the enthalpy equations for the test gas mixtures used herein. The enthalpy equations used herein were based on data extracted from NASA SP-3001 (Ref 12). The theoretical curves of T_5/T_1 versus M for the three test gas mixtures used in this study are shown in Figs 3, 4, and 5. The computer generated values of T_5/T_1 versus M used to plot these curves are tabulated in Appendix B.

To obtain T_5 , the incident shock wave Mach number was first calculated. At this value of M , the ratio T_5/T_1 was extracted from the graphs of Figs 3, 4, or 5. Hence

$$T_5 = (T_5/T_1)(T_1)$$

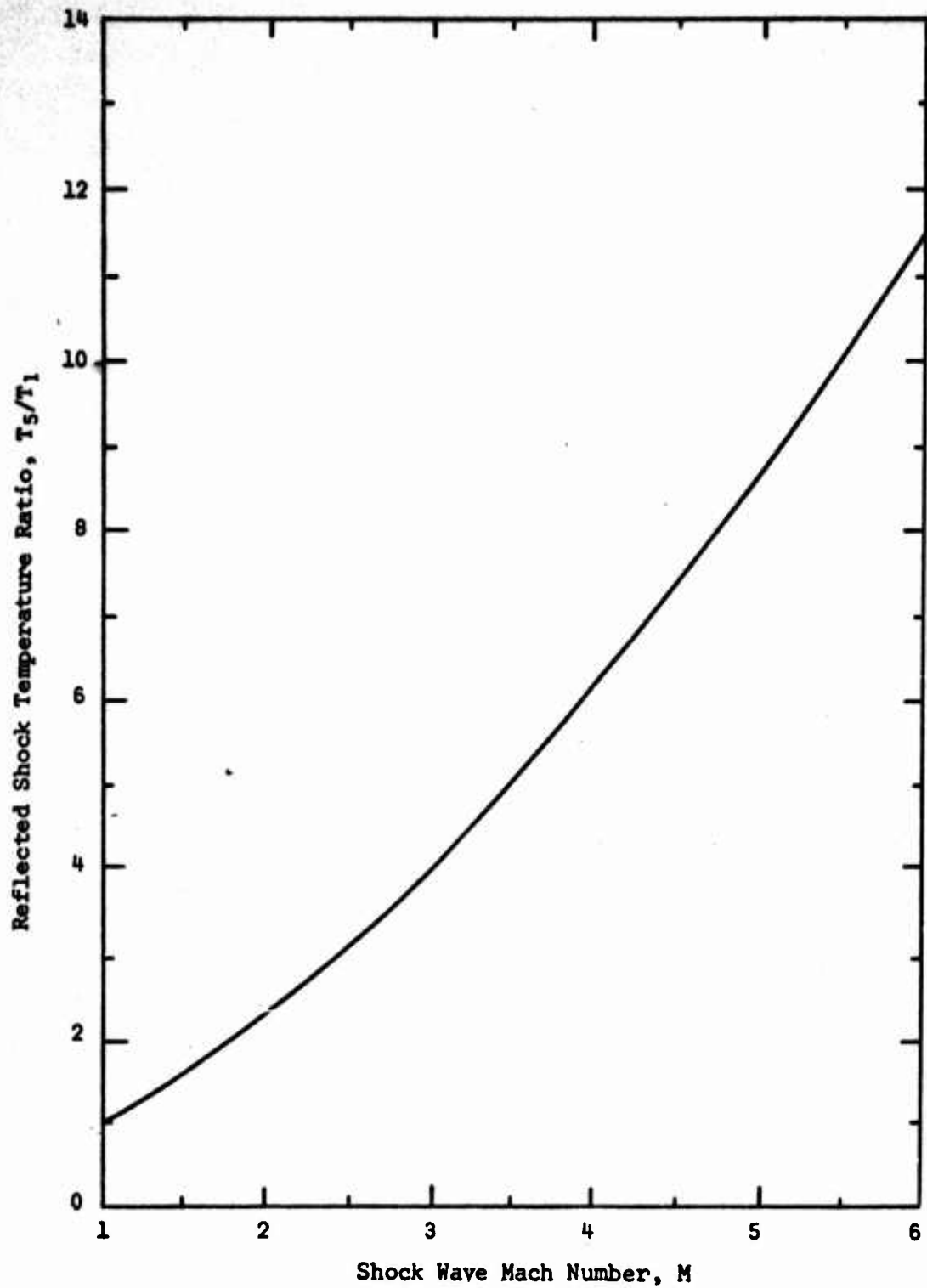


Figure 3. Reflected Shock Temperature Ratio for 60% N_2 , 20% CO , 20% N_2O

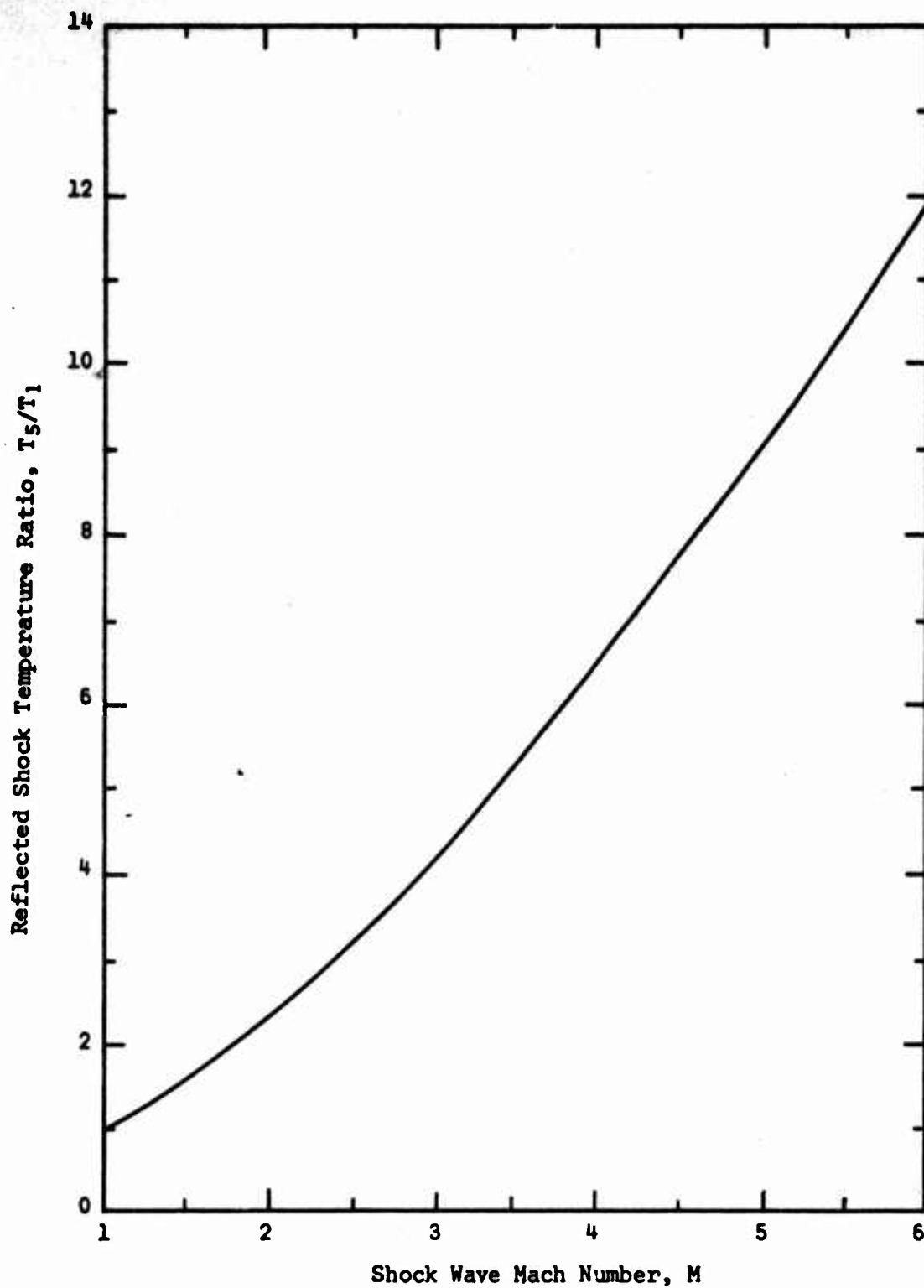


Figure 4. Reflected Shock Temperature Ratio for
70% N_2 , 15% CO , 15% N_2O

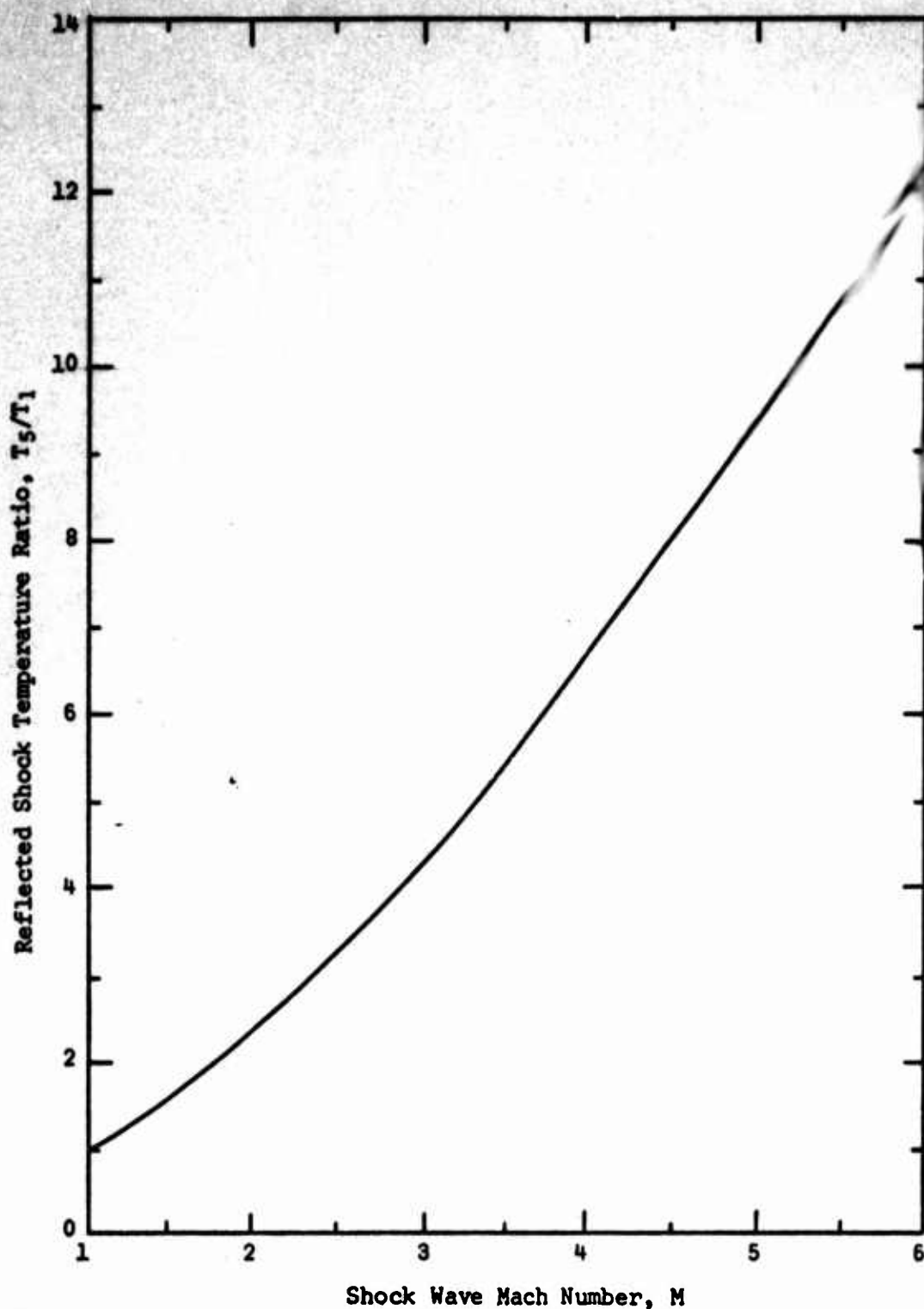


Figure 5. Reflected Shock Temperature Ratio for
80% N_2 , 10% CO , 10% N_2O

Reflected Shock Pressure, P_5

The reflected shock pressure was obtained by two methods, one acting as a check on the other. The first method was theoretical. In this method, theoretical curves for P_5/P_1 versus M for the three test gas mixtures were obtained from the same modified computer program which generated the theoretical T_5 values for equilibrium test gas mixtures. First, the incident shock wave Mach number was calculated. At this value of M , the ratio P_5/P_1 was extracted from the graphs of Figs 6, 7, or 8. The computer generated values of P_5/P_1 versus M used to plot these curves are tabulated in Appendix B. Hence

$$P_5 = (P_5/P_1)(P_1)$$

where P_1 was the initial pressure in the driven section.

The second method was experimental. In this method, the reflected shock pressure was determined from the oscilloscope pressure trace. A diagram of an oscilloscope trace for a test run without ignition is shown in Fig 9. The line across the top represents the output trace of the photomultiplier tube which indicates no ignition. The light emitted due to combustion causes a downstep of this trace (increasing downward). The pressure trace shows both the incident and reflected shock pressure steps (increasing upward). A photograph of a representative no-ignition run is shown in Fig 10.

The distance corresponding to $P_5 - P_1(\Delta h)$ was measured from the photograph. Then using the instrumentation scale settings, P_5 was found by:

$$P_5 = P_1 + \frac{\Delta h(V.V.S.)}{V.P.F.}$$

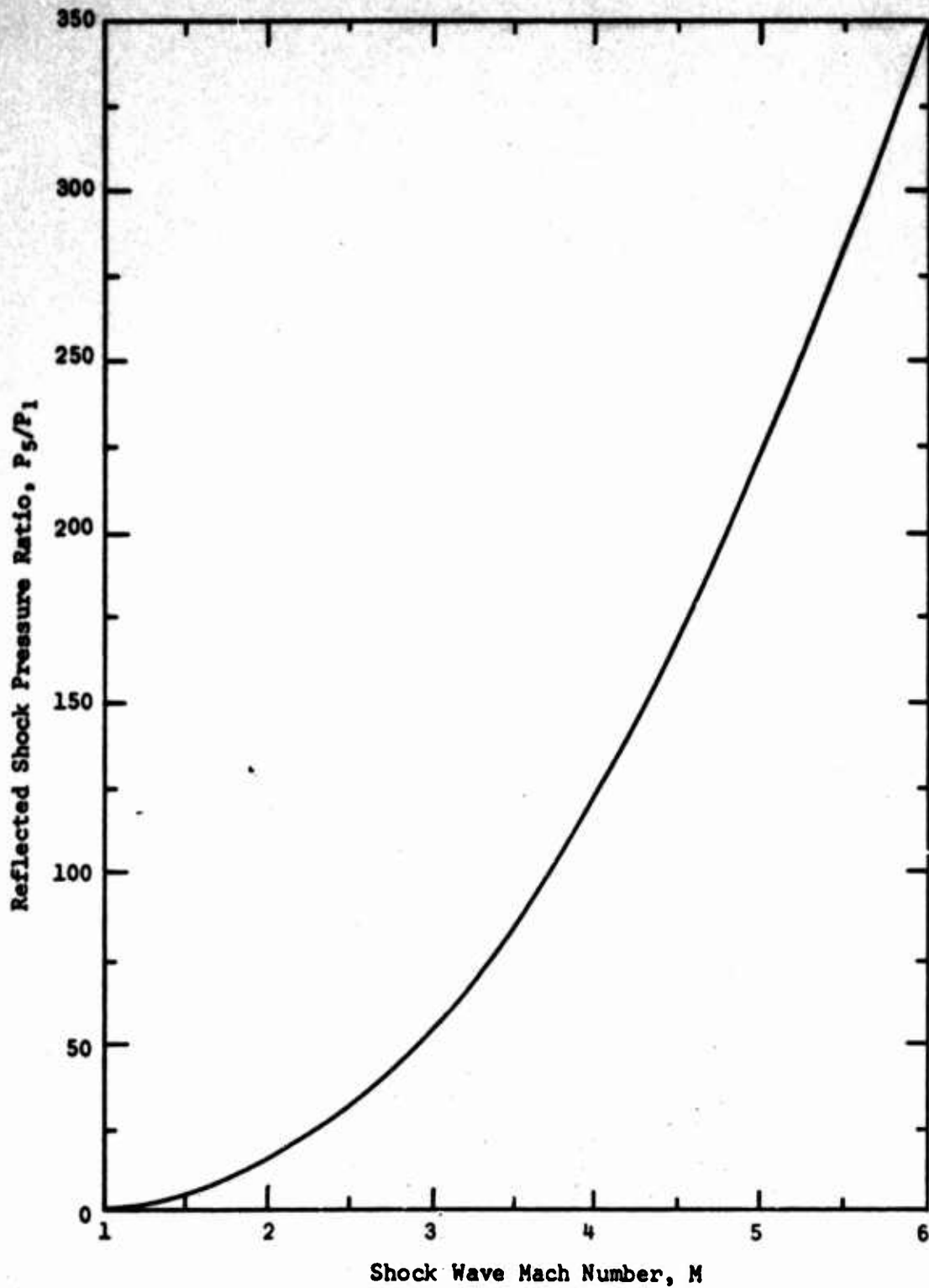


Figure 6. Reflected Shock Pressure Ratio for 60-20-20

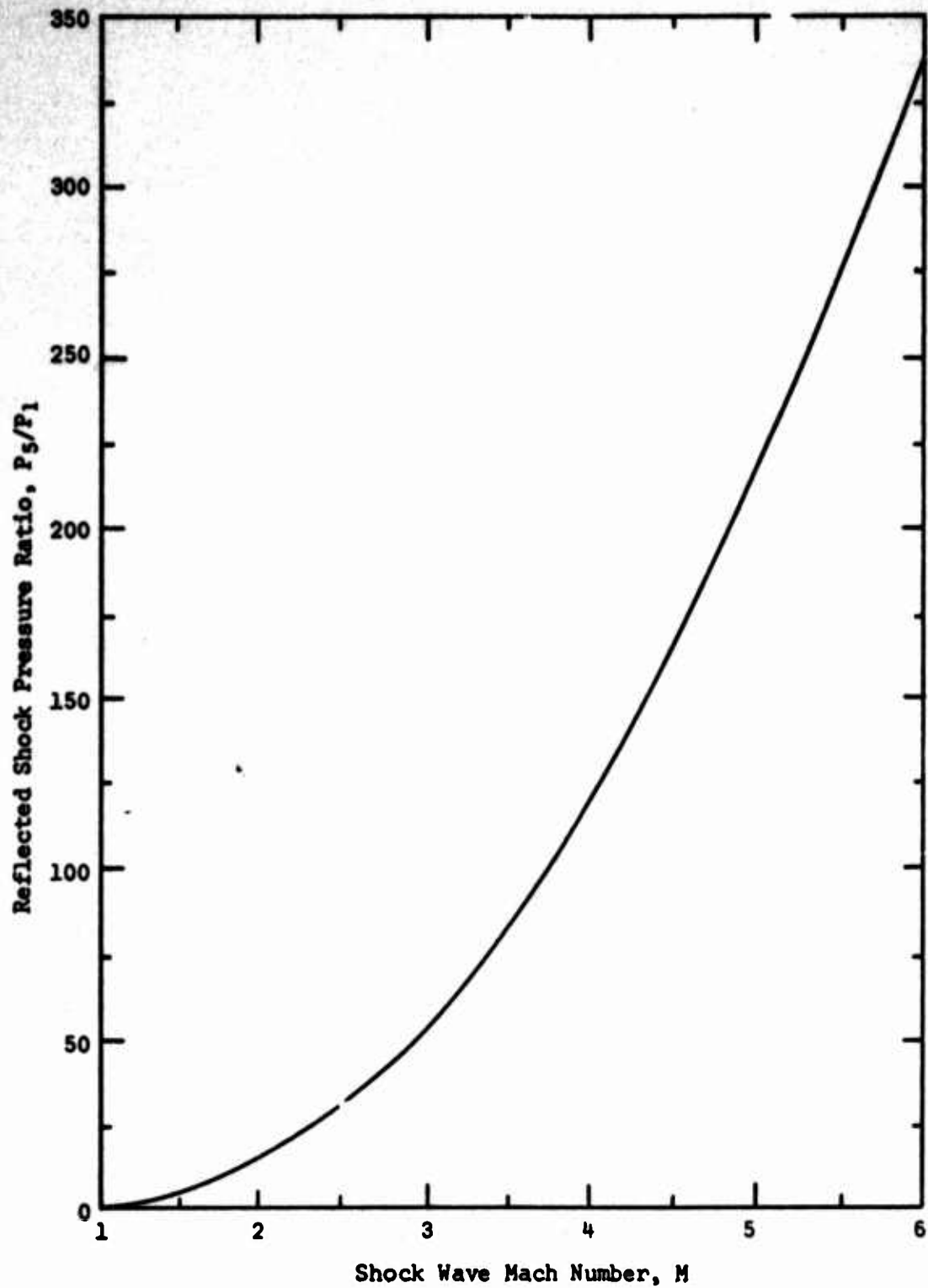


Figure 7. Reflected Shock Wave Pressure Ratio for 70-15-15

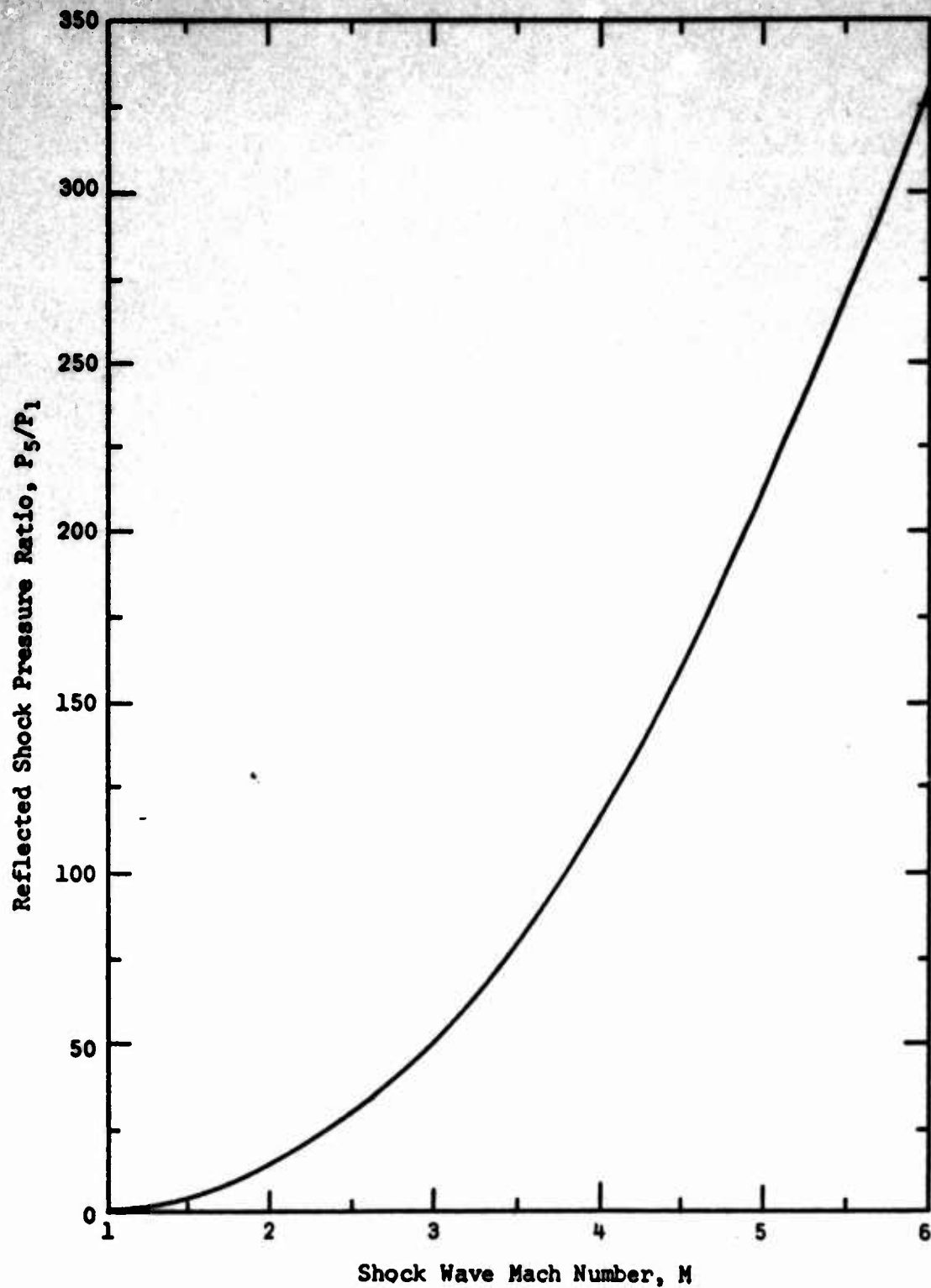


Figure 8. Reflected Shock Wave Pressure Ratio for 80-10-10

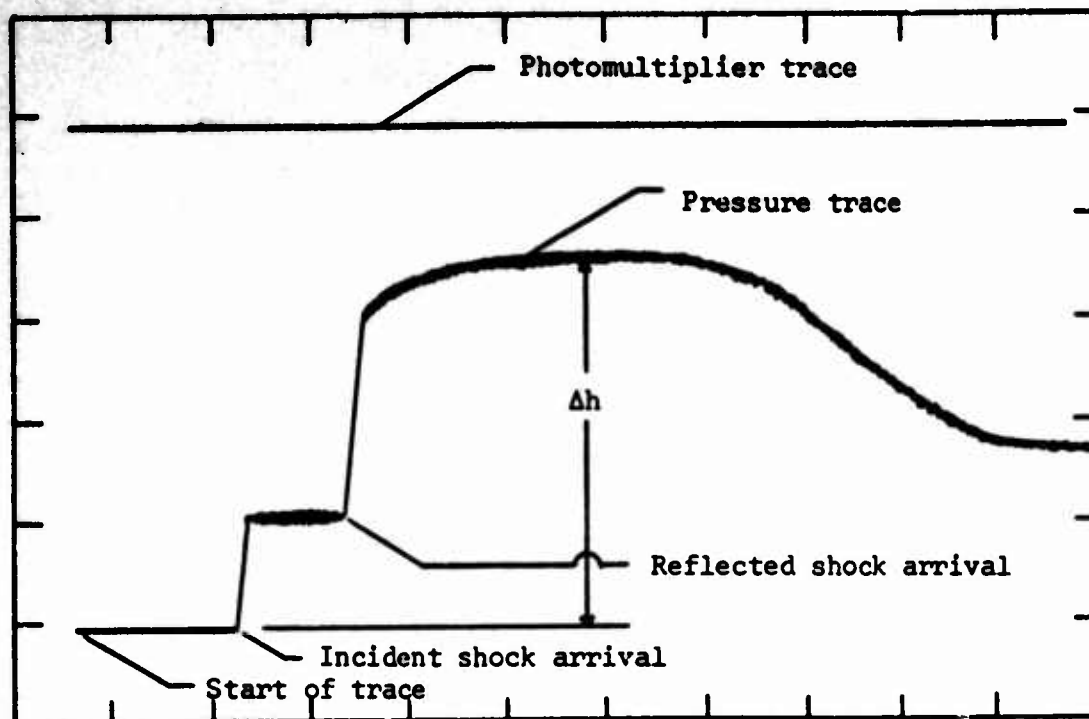
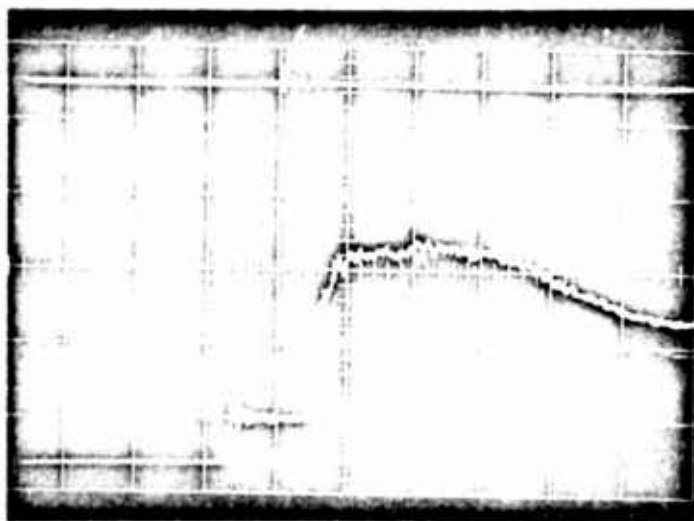


Figure 9. Diagram of Oscilloscope Trace for Test Run Without Ignition



Run 30A-3
 $M = 2.44$
 $T_5 = 930^\circ K$
 $P_5 = 4.9 \text{ atm}$
 $V.V.S. = 500 \text{ mv/cm}$
 $V.P.F. = 23.2 \text{ mv/psia}$
 $V.T.S. = 0.5 \text{ msec/cm}$

Figure 10. Photograph of Oscilloscope Trace for a Test Run Without Ignition

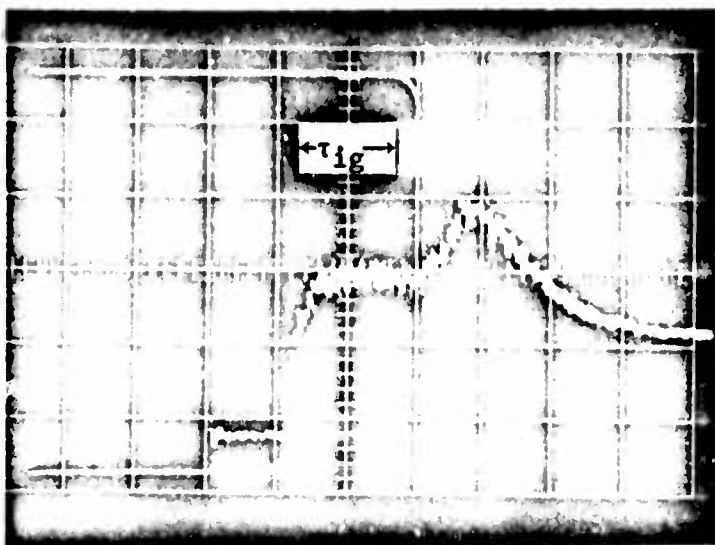
Uda (Ref 13) found in his shock tube study of boron particles igniting in air that the theoretical value of P_5 corresponded very closely to the experimental values. In his study, Uda used Craig's unmodified computer program to generate a P_5/P_1 versus M curve and T_5/T_1 versus M curve.

Ignition Delay Time, τ_{ig}

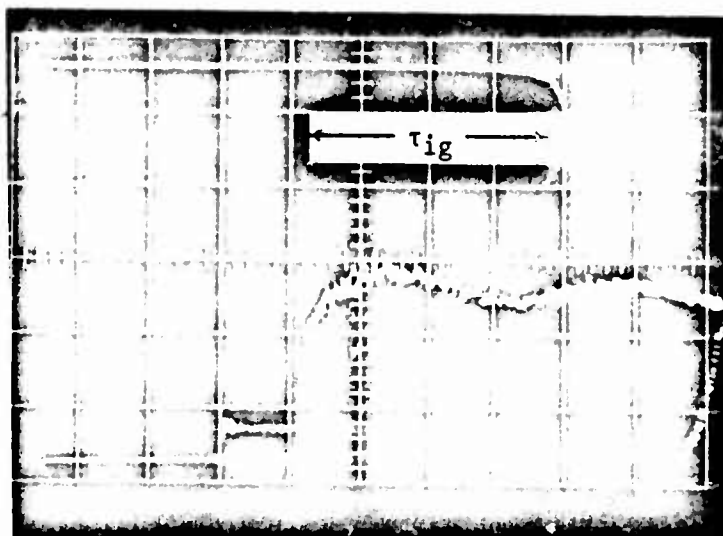
When ignition of the N_2O , CO , N_2 gas mixture occurs in the test section, the photomultiplier trace on the photograph shows a downstep, indicating light output and ignition. The pressure trace in the reflected shock region correspondingly rises when ignition occurs. Herein, the time interval between the beginning of the reflected shock pressure step and the beginning of the photomultiplier downstep is defined as the ignition delay time. Two tests showing different ignition delay times are presented in Fig 11.

Ignition delay time was determined experimentally by the relation

$$\tau_{ig} = \Delta w(V.T.S.)$$



Run 24A-5

 $M = 2.83$ $T_5 = 1107^\circ K$ $P_5 = 62.6 \text{ atm}$ $V.V.S. = 2000 \text{ mv/cm}$ $V.P.F. = 5.8 \text{ mv/psia}$ $V.T.S. = 0.5 \text{ msec/cm}$ 

Run 22A-9

 $M = 2.88$ $T_5 = 1134^\circ K$ $P_5 = 16.7 \text{ atm}$ $V.V.S. = 1000 \text{ mv/cm}$ $V.P.F. = 11.6 \text{ mv/psia}$ $V.T.S. = 0.5 \text{ msec/cm}$

Figure 11. Photographs of Two Test Runs with Different Ignition Delay Times

V. Discussion of Results

A shock tube was used to establish the ignition limit curves for three mixtures of N_2 , CO, and N_2O . The test gas mixtures were self-ignited behind the reflected shock wave. The ignition limit curves were determined for pressures ranging from 5 to 65 atm. Additionally, information on ignition delay time was obtained for each of the three mixtures.

Flame Spectrum Analysis

A flame holder was set up to determine the flame spectrum from igniting N_2O and CO (Fig 12). A Fisher burner was modified by adding a donut-shaped, metal container which completely enclosed the normal air intake ports. Two additional base connectors were welded to this metal container so that three gases could be fed into the Fisher burner simultaneously and ignited as a flame at the top of the burner. The bottles of N_2O , CO, and N_2 were each connected to a separate nozzle on the Fisher burner and each gas flow was controlled by a pressure regulator. The CO was flowed first and ignited with atmospheric air by a striker. The N_2O was then flowed into the Fisher burner at the same flow rate as the CO and the CO and N_2O then ignited together. When the CO was first ignited with the striker, the characteristic deep blue "CO-flame" was visible. As the N_2O was added to the CO, the flame changed very noticeably to that of a bright, pinkish white. Adding the N_2 simply diluted the flame and finally extinguished it as the flow of N_2 was increased.

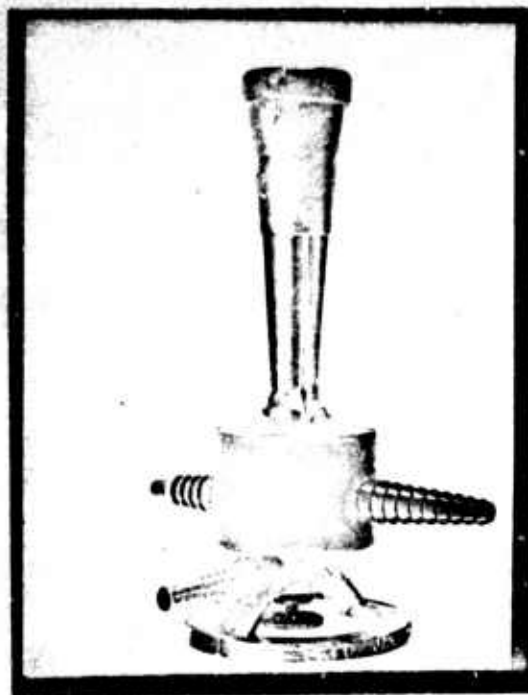


Figure 12. Modified Fisher Burner for Flame Spectrum Analysis

To avoid extraneous light from entering the monochrometer, this flame test was performed at night with minimum light available. The monochrometer showed that the N_2O , CO , N_2 flame spectrum extended from 3000 to 6000 \AA , i.e., a continuum. Kaskan showed that this spectrum is radiated by any flame containing CO and O and arises from the reaction of $\text{CO} + \text{O}$ (Ref 14). This spectrum was scanned using the monochrometer until the maximum signal was indicated on the oscilloscope screen. This setting was 5300 \AA and the monochrometer was not reset from this value for the remainder of the study. This setting of 5300 \AA gave good indication that the N_2O and CO had reacted in the test section, as evidenced by the photomultiplier downsteps in Fig 11.

Ignition Limit

The ignition temperature limit curves of three gas mixtures of N_2O , CO , and N_2 are shown in Figs 13, 14, and 15 where the reflected shock temperature T_5 is plotted versus the reflected shock pressure P_5 . Data were obtained at constant values of P_1 (initial pressure of the test gas in the driven section) until the ignition limit point was established in each case. A line was then constructed through the data points to approximate the ignition limit curve, i.e., to separate the ignition and no-ignition zones.

As can be seen in Fig 13, the ignition limit curve for the 60% N_2 , 20% CO , 20% N_2O mixture decreases linearly from about 1120°K at 5 atm to about 1000°K at 65 atm. The ignition limit curve for the 70% N_2 , 15% CO , 15% N_2O mixture in Fig 14 decreases linearly from about 1145°K at 5 atm to about 1060°K at 65 atm. This decrease in ignition temperature for the 70-15-15 mixture is at a lesser rate than that for

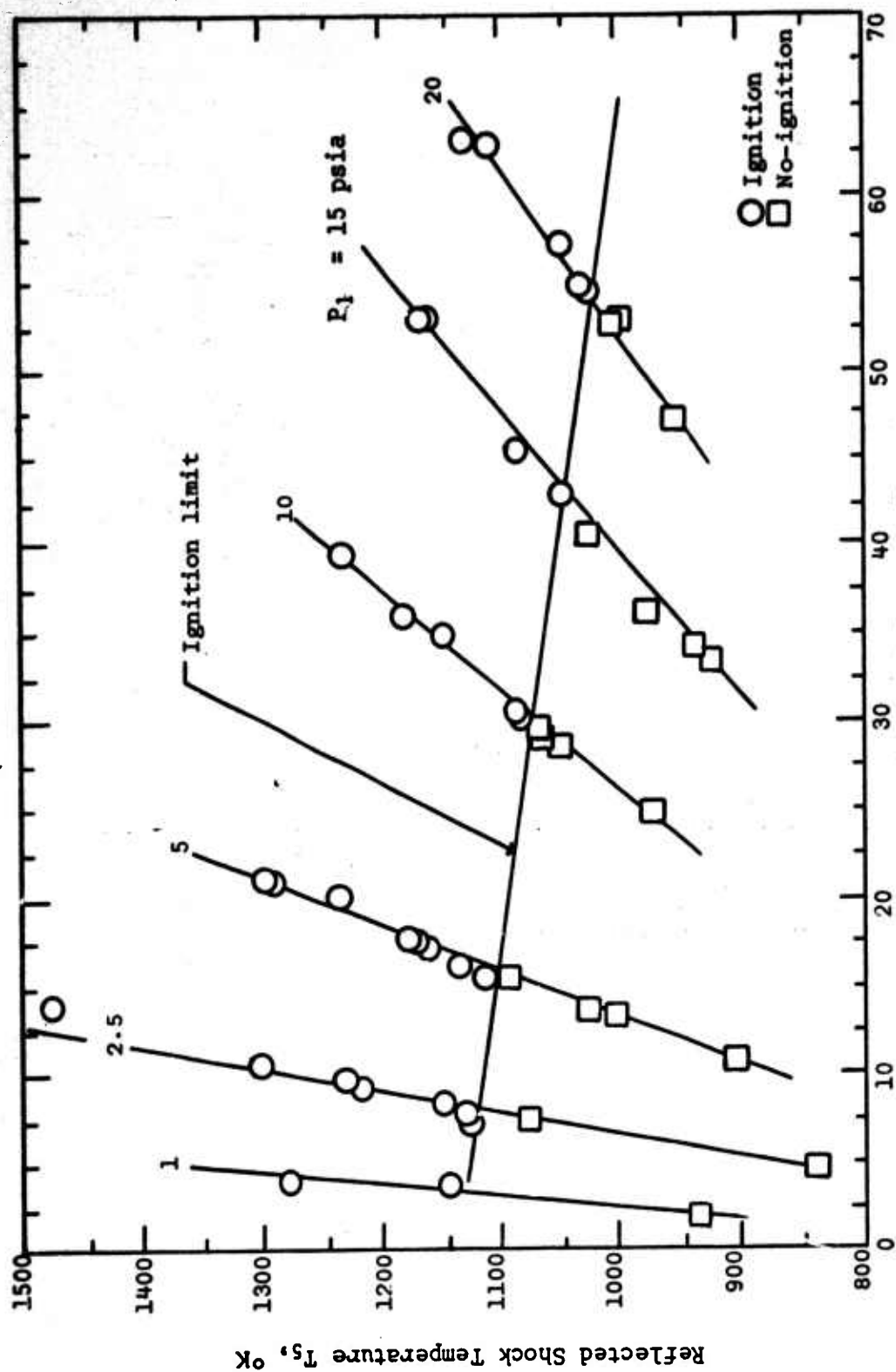


Figure 13. Ignition Limit Curve for 60-20-20 Mixture Ignited Behind a Reflected Shock Wave

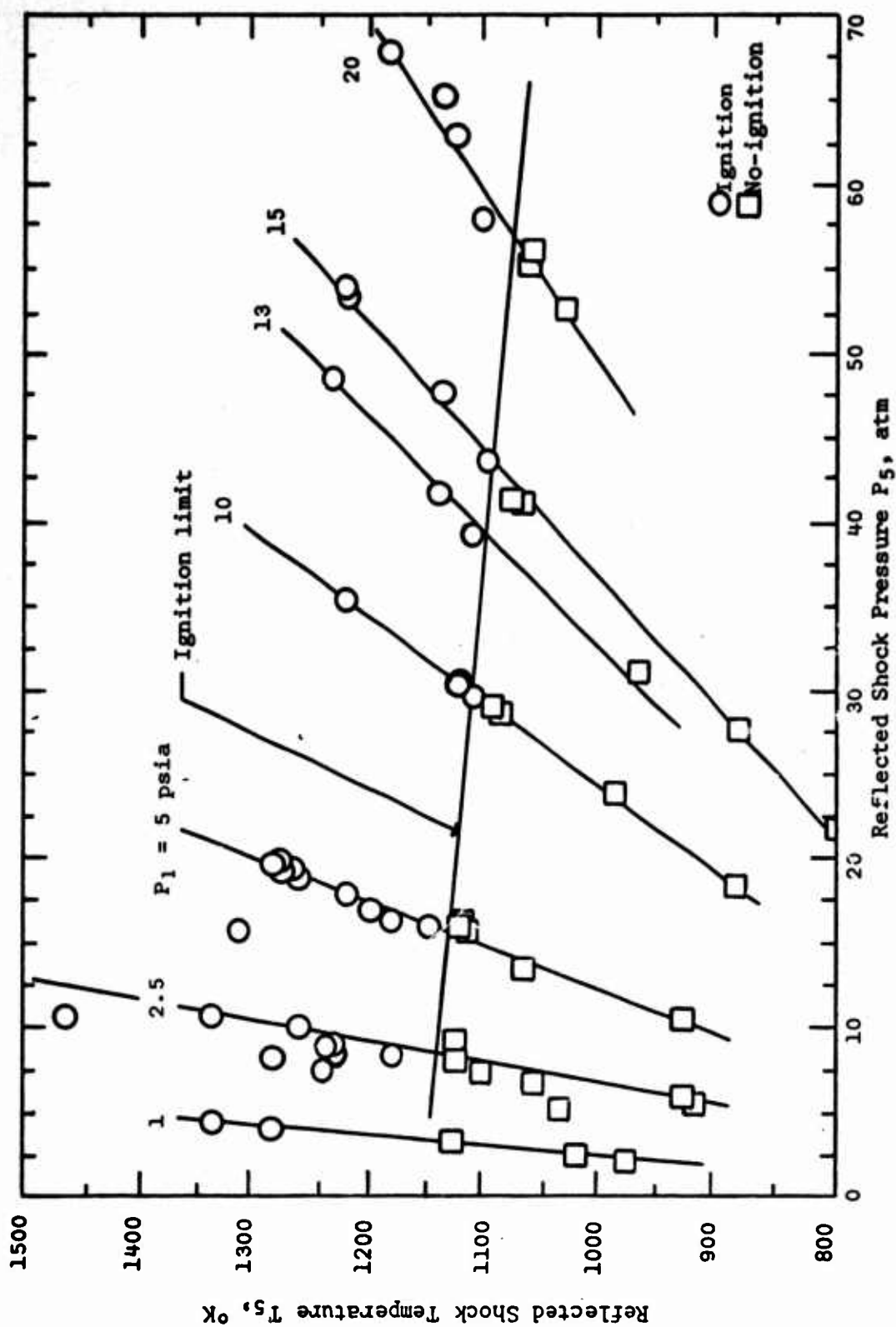


Figure 14. Ignition Limit Curve for 70-15-15 Mixture Ignited Behind a Reflected Shock Wave

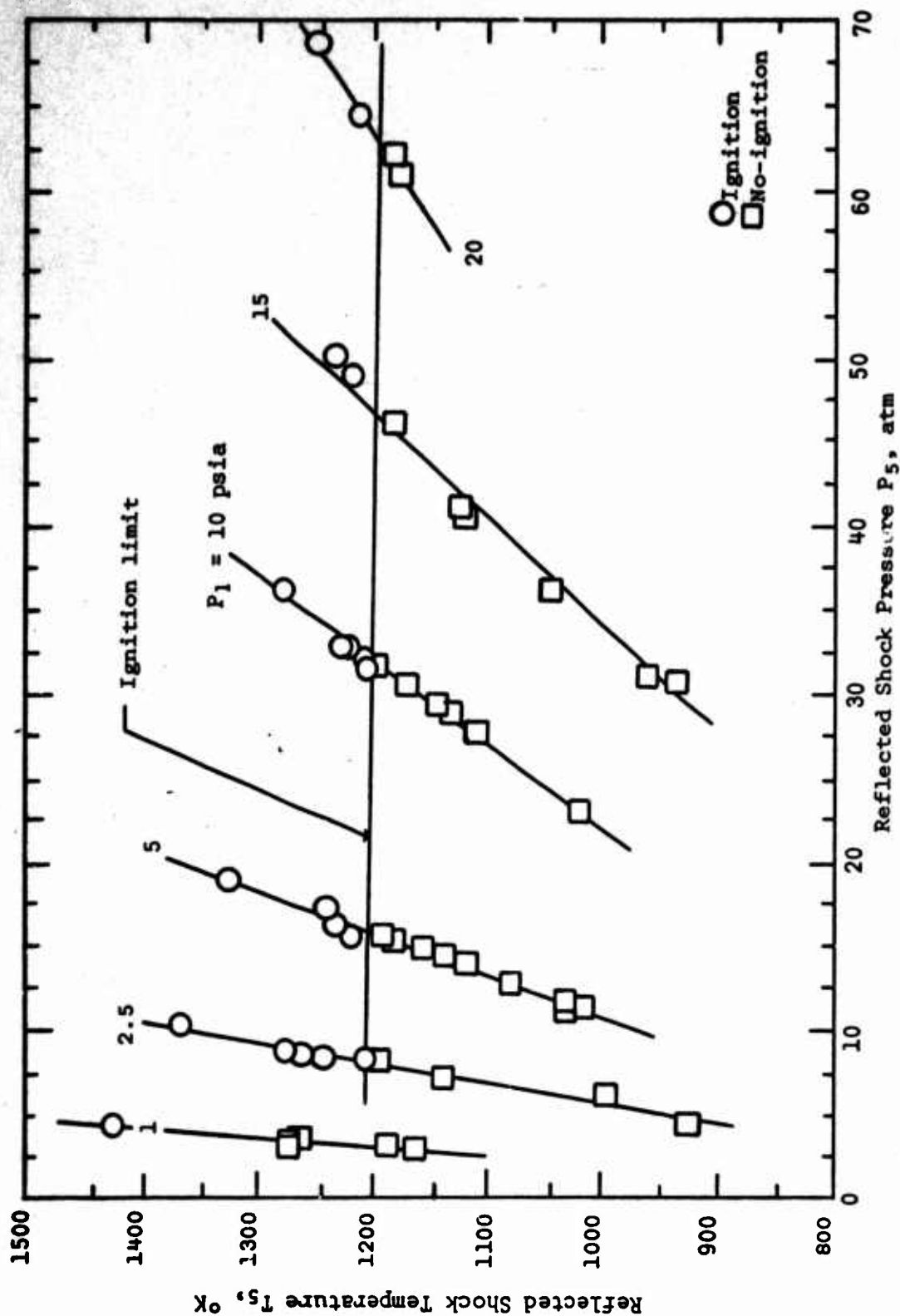


Figure 15. Ignition Limit Curve for 80-10-10 Mixture Ignited Behind a Reflected Shock Wave

the 60-20-20 mixture. As can be seen in Fig 15, the ignition temperature of the 80% N_2 , 10% CO, 10% N_2O mixture decreases linearly and very slightly with increasing pressure from about 1210°K at 5 atm to about 1200°K at 65 atm. At the lower pressure end of the 80-10-10 mixture (<5 atm), it appears that the ignition limit increases rapidly to a temperature above 1300°K. However, further tests must be conducted to substantiate this speculation.

The results of this study for the ranges of pressures considered show that the ignition temperature is dependent on the amount of CO and N_2O present, i.e., the greater the amount of CO and N_2O in the mixture, the lower the ignition temperature. It also appears that the ignition temperature is dependent on pressure as the amount of CO and N_2O is increased in the mixture. Although Lin and Bauer did not evaluate stoichiometric mixtures of N_2O and CO in their study, their data did indicate a similar decrease in ignition temperature with increasing amounts of N_2O and CO in the test mixture.

Ignition Delay Time

Herein, ignition delay time is defined as the time interval between the beginning of the reflected shock pressure step and the beginning of the photomultiplier downstep (Fig 11). The results for ignition delay time are presented in Figs 16, 17, and 18. The curves represent the average of three or more data points which had nearly the same P_5 values. A pressure-temperature correlation does exist for each gas mixture. The effect of increasing pressure at a given temperature is to reduce the ignition delay time. A similar effect occurs

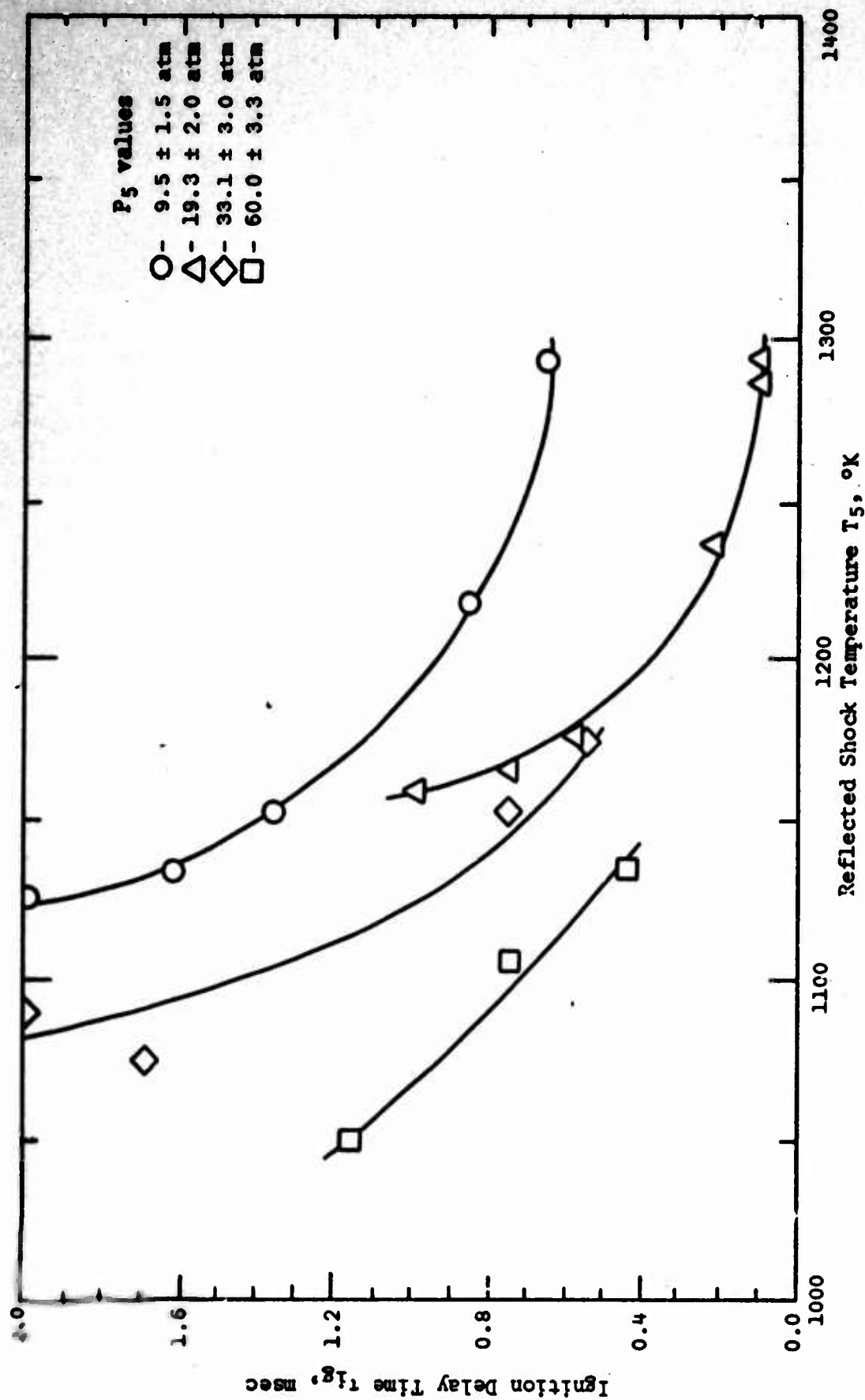


Figure 16. Ignition Delay Time for 60-20-20 Mixture Ignited Behind a Reflected Shock Wave

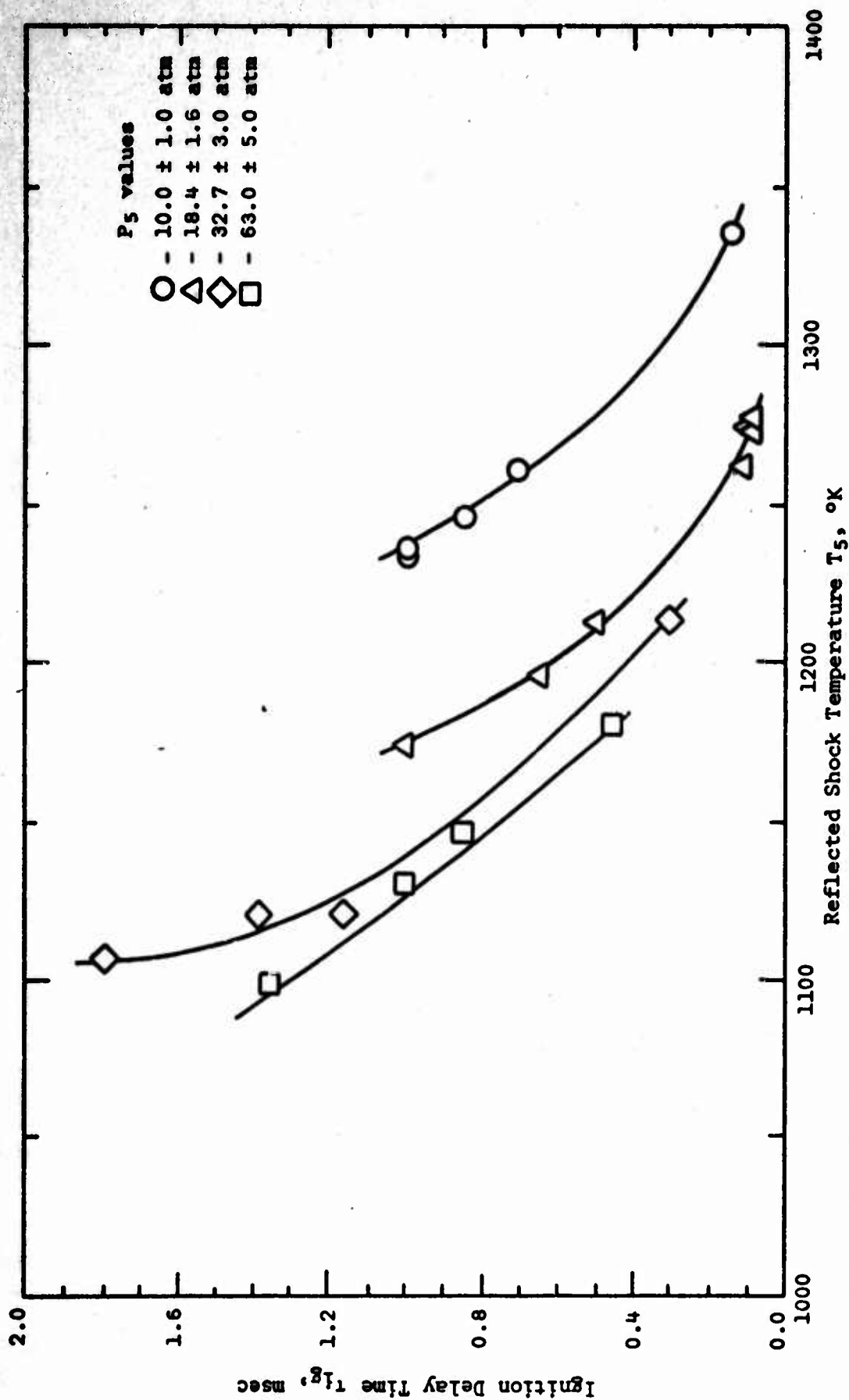


Figure 17. Ignition Delay Time for 70-15-15 Mixture Ignited Behind a Reflected Shock Wave

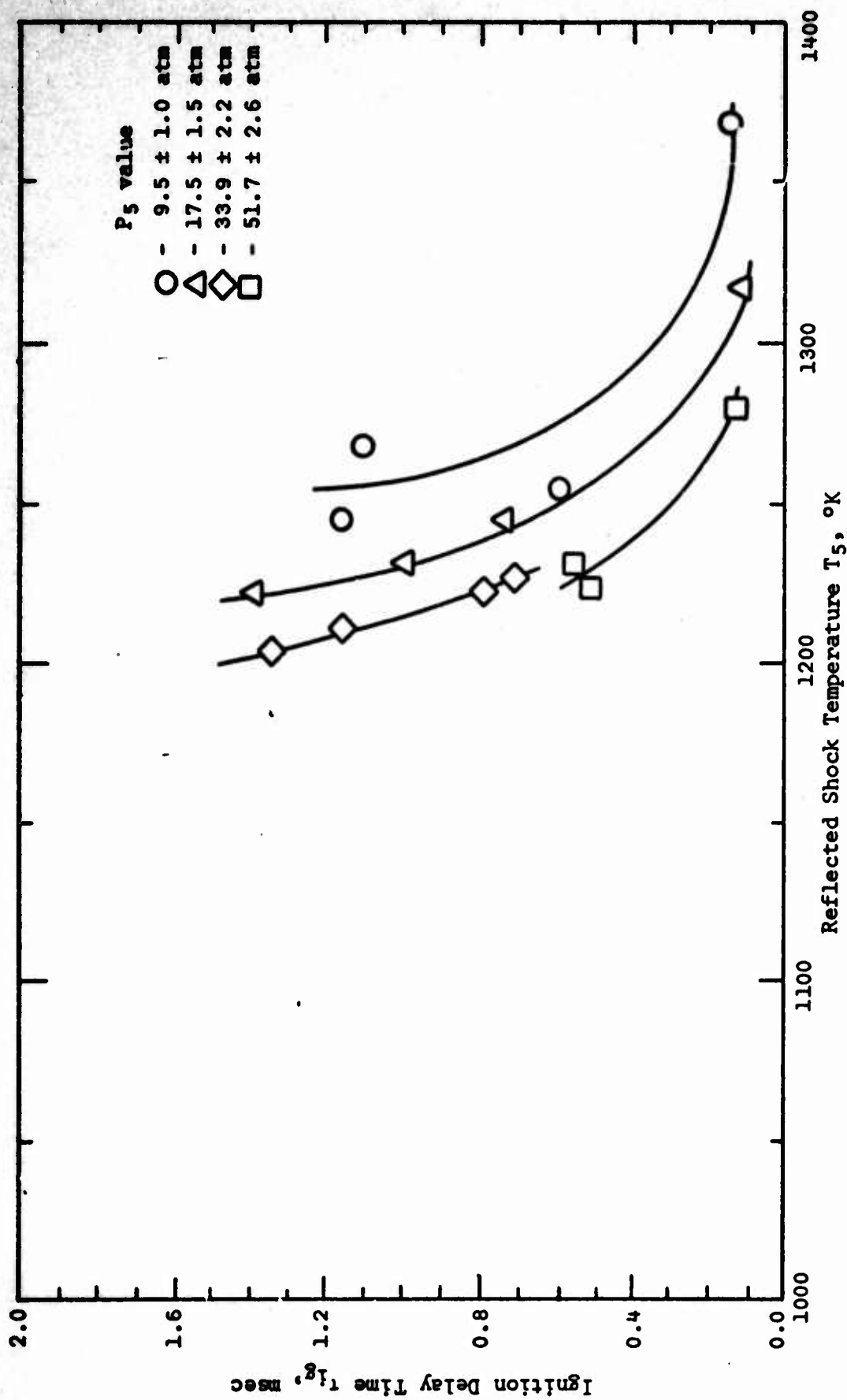


Figure 18. Ignition Delay Time for 80-10-10 Mixture Ignited Behind a Reflected Shock Wave

whenever the temperature is increased at a given pressure. This correlation was shown to be true for gas-gas mixtures of hydrogen-air by Craig (Ref 11).

The effect of increasing the amount of N_2O and CO present in the test gas mixture is to decrease ignition delay time for a given pressure, P_5 . It should be noted that due to the oscilloscope time sweep scale used in this study the ignition delay time could not be read below 0.10 msec. Any ignition delay time less than 0.10 msec appeared to be instantaneous on the oscilloscope photographs and was plotted as 0.10 msec. It should also be noted that any influence on the reaction by the oxygen remaining in the evacuated driven section was not considered in this study. Although the driven section was evacuated to about 0.5 mm Hg before each test run, there remained 0.5 mm Hg of air and subsequently 0.01 mm Hg of oxygen in the driven section.

VI. Conclusions and Recommendations

Ignition limit curves for three gas mixtures of 60% N_2 , 20% CO, 20% N_2O ; 70% N_2 , 15% CO, 15% N_2O ; and 80% N_2 , 10% CO, 10% N_2O have been determined for pressures ranging from 5 atm to 65 atm. A shock tube was employed to ignite the test gas mixtures behind the reflected shock wave. Ignition delay time data were also obtained for the three gas mixtures.

Conclusions

The results of this study allow the following conclusions to be drawn.

1. The ignition temperature for the N_2 , CO, N_2O gas mixtures decreases linearly as pressure increases. The ignition temperature is a function of the amount of N_2O and CO present in the test gas mixture.
2. The ignition temperature is more dependent on pressure (for the range tested) as the amount of CO and N_2O is increased in the mixture.
3. Ignition delay time is reduced by increasing the pressure at a given temperature or increasing the temperature at a given pressure.
4. Ignition delay time is decreased by increasing the amount of N_2O and CO present in the test gas at a given pressure (in the range tested).

Recommendations

Based on the results of this study, the following recommendations are proposed:

1. Studies should be extended to several other gas mixture compositions of N_2O , CO , and N_2 so that a definite correlation can be established between varying amounts of N_2O and CO present in the mixture with temperature and pressure.

2. Similar tests as those described in this study should be performed to substantiate the assumption that the ignition limit increases sharply to above $1300^\circ K$ for the 80% N_2 , 10% CO , 10% N_2O mixture and possibly others for pressures less than 5 atm.

3. Tests similar to those completed herein be made for the gas mixtures used herein but with more control over the amount of oxygen that remains in the driven section after evacuation. Evacuation to less than 0.50 mm Hg should be attempted to reduce the amount of remaining oxygen.

4. Tests similar to those completed herein be made for the gas mixture used herein but with gases of greater purity. Any effect that impurities might have on the ignition temperature and/or ignition delay time would be of interest.

5. More detailed ignition delay studies should be conducted to gather additional information on the correlation with changes of pressure, temperature, and gas mixture composition.

Bibliography

1. Van Wontergham, J. and A. Van Tiggelen. "Flame Propagation in Gaseous Mixtures Containing Nitrous-Oxide as Oxidant." Bulletin of the Belgium Chemical Society, 64:780-797, September 1955.
2. Lin, M.C. and S.H. Bauer. "Bimolecular Reaction of N_2O with CO and the Recombination of O and CO as Studied in a Single-Pulse Shock Tube." The Journal of Chemical Physics, 50:3377-3391, 15 April 1969.
3. Soloukhin, R.I. "High-temperature Oxidation of Ammonia, Carbon Monoxide, and Methane by Nitrous Oxide in Shockwaves." Thirteenth Symposium (International) on Combustion. Pittsburgh: The Combustion Institute, 1971.
4. Gaydon, A.G. and I.R. Hurle. The Shock Tube in High Temperature Chemical Physics. New York: Reinhold Publishing Corporation, 1963.
5. Glass, I.I. Shock Tubes, Part 1. Toronto: University of Toronto Institute of Aerophysics, May 1958.
6. Greene, E.F. and P.J. Toennies. Chemical Reactions in Shockwaves. New York: Academic Press, 1964.
7. Hall, G.J. Shock Tubes, Part II. Toronto: University of Toronto Institute of Aerophysics, May 1958.
8. Rudinger, G. Wave Diagrams for Non-Steady Flow in Ducts. New York: D. Van Nostrand Company, Inc., 1955.
9. Wright, J.K. Shock Tubes. London: Methruen and Co., Ltd, 1961.
10. Caponecchi, A.J. The Design and Construction of a Chemical Shock Tube. Unpublished Thesis. Wright-Patterson AFB, Ohio: Air Force Institute of Technology, June 1967.
11. Craig, R.R. A Shock Tube Study of the Ignition Delay of Hydrogen-Air Mixtures Near the Second Explosion Limit. Technical Report AFAPL-TR-66-74. Wright-Patterson AFB, Ohio: Air Force Aero Propulsion Laboratory, November 1966.
12. McBride, B.J., S. HeimeI, J. Ehlers, and S. Gordon. Thermodynamic Properties to 6000°K for 210 Substances Involving the First 18 Elements. NASA SP-3001. Washington: National Aeronautics and Space Administration, March 1963.

13. Uda, R.T. A Shock Tube Study of the Ignition Limit of Boron Particles. Unpublished Thesis. Wright-Patterson AFB, Ohio: Air Force Institute of Technology, June 1968.
14. Kaskan, W.E. "The Source of the Continuum in Carbon Monoxide-Hydrogen-Air Flames." Combustion & Flame, 3:39-48, 1959.

Appendix A

Test Data

The reduced data which were used to plot the graphs for Figs 13 through 18 are tabulated in this appendix.

Table I

Ignition limit data for 60% N₂, 20% CO, 20% N₂O (Fig 13)

Run Number	T ₅ (°K)	P ₅ (atm)	Ignition	
			Yes	No
21A-3	1143	3.4	x	
-4	1278	4.1	x	
-5	840	4.6		x
-7	1233	9.9	x	
-8	1293	10.6	x	
-9	1473	13.9	x	
-10	1221	9.4	x	
-11	906	10.7		x
-12	1107	15.6	x	
-13	1239	20.1	x	
-14	1287	21.1	x	
22A-1	975	24.4		x
-2	1065	29.8		x
-3	1065	29.9		x
-4	1056	28.6		x
-5	1089	30.6	x	
-6	1176	36.1	x	
-7	1233	39.5	x	
-8	1032	13.7		x
-9	1134	16.7	x	
23A-1	945	34.7		x
-2	1089	45.9	x	
-3	1050	42.8	x	
-4	1164	53.0	x	
-5	1164	53.0	x	
-6	1134	63.3	x	
24A-1	1029	54.4	x	
-3	1002	53.1		x
-4	1050	57.0	x	

Table I (continued)

Run Number	T ₅ (°K)	P ₅ (atm)	Ignition	
			Yes	No
24A-5	1107	62.6	x	
-6	1158	17.3	x	
27A-2	1134	8.3	x	
-3	1152	8.6	x	
-4	999	12.9		x
-5	1176	18.0	x	
-6	1074	30.1	x	
-7	1152	34.2	x	
28A-1	1293	21.3	x	
-2	1032	54.7	x	
13S-3	1125	8.1	x	
-4	1074	7.5		x
-5	1164	17.5	x	
-6	1089	15.3		x
-7	921	33.7		x
-8	975	36.5		x
-9	1029	40.8		x
-10	960	47.6		x
-11	1014	53.1		x
-12	942	2.4		x

Table II

Ignition limit data for 70% N₂, 15% CO, 15% N₂O (Fig 14)

Run Number	T ₅ (°K)	P ₅ (atm)	Ignition	
			Yes	No
6A-1	1125	9.4		x
7A-1	1305	16.0	x	
8A-1	1104	39.3	x	
-2	1119	30.6	x	
10A-1	885	18.7		x
-2	981	23.8		x
-3	1212	35.7	x	
-4	1086	28.6		x
-5	1119	30.6	x	
-6	1311	41.9	x	
-8	772	21.2		x
-9	798	22.4		x
-10	870	27.6		x
-11	960	30.9		x
-12	1065	40.8		x
13A-3	939	10.5		x
-4	1116	15.9		x
-5	1116	15.9		x
14A-1	1278	19.7	x	
-2	1275	19.4	x	
-3	1212	17.9	x	
-4	1260	19.4	x	
-5	930	5.3		x
-6	939	5.3		x
15A-1	1236	9.4	x	
-2	1335	10.7	x	
-3	1236	9.4	x	
-4	1173	16.8	x	
-5	1092	28.9		x
16A-1	1104	29.8	x	
-2	1068	41.3		x
-3	1224	53.8	x	
-4	1224	53.8	x	
-5	1236	48.6	x	
-6	1140	41.4	x	
-7	1098	43.5	x	
17A-2	1281	8.0	x	
-3	1035	5.3		x
-4	1125	3.2		x
-5	1335	4.3	x	
-6	1140	47.6	x	
-7	1029	52.6		x
-8	1059	56.2		x

Table II (continued)

Run Number	T ₅ (°K)	P ₅ (atm)	Ignition	
			Yes	No
21A-1	1245	7.5	x	
-2	1464	10.5	x	
10S-1	972	2.3		x
-2	1059	6.8		x
-3	1125	7.8		x
-4	1245	9.4	x	
-5	1260	10.0	x	
-6	1098	7.3		x
-7	1173	8.4	x	
-8	1110	15.9		x
11S-1	1194	17.3	x	
-2	1275	20.0	x	
12S-1	1260	19.4	x	
-2	1065	13.6		x
-3	1182	68.0	x	
-4	1146	65.3	x	
-5	1068	55.1		x
-6	1098	58.1	x	
-7	1146	16.3	x	
-8	1131	63.1	x	
13S-1	1020	2.6		x
-2	1281	4.0	x	

Table III

Ignition limit data for 80% N₂, 10% CO, 10% N₂O (Fig 15)

Run Number	T ₅ (°K)	P ₅ (atm)	Ignition	
			Yes	No
29A-1	1161	3.0		x
-2	1269	3.5		x
-4	1368	10.3	x	
-5	1269	8.8	x	
-6	1128	28.5		x
-7	1275	36.1	x	
30A-1	1254	8.6	x	
-2	1245	8.5	x	
-3	930	4.9		x
-4	1008	11.6		x
-5	1041	12.2		x
-6	1236	16.7	x	
-7	1119	13.8		x
-8	1221	16.3	x	
-9	1317	19.0	x	
-10	1041	11.9		x
-11	1014	23.0		x
-12	1221	32.7	x	
31A-1	1149	29.3		x
-2	1206	32.4	x	
-3	939	30.3		x
-4	963	30.8		x
-5	1050	36.7		x
-6	1122	41.6		x
-7	1185	46.7		x
-8	1236	50.1	x	
-9	1122	41.6		x
-10	1149	43.9		x
-11	1281	54.3	x	
-12	1122	41.6		x
-13	1221	49.1	x	
-14	1176	61.2		x
4S-1	786	3.4		x
-2	1080	12.9		x
-3	1194	8.0		x
6S-1	1143	14.5		x
-2	1161	15.0		x
-3	1176	15.3		x
-4	1245	17.1	x	
-5	1227	33.0	x	
-6	1113	27.4		x
-7	1203	31.7	x	
-8	1206	8.1	x	

Table III (continued)

Run Number	T ₅ (°K)	P ₅ (atm)	Ignition	
			Yes	No
6S-9	1095	6.7		x
-10	1425	4.4	x	
-11	1269	3.0		x
-12	1194	32.0		x
7S-1	1185	15.6		x
-2	1185	3.1		x
-3	1185	62.3		x
-4	1206	64.8	x	
-5	1254	68.6	x	
-8	1143	7.3		x
-9	1167	30.2		x

Table IV

Ignition delay data for 60% N₂, 20% CO, 20% N₂O (Fig 16)

T ₅ (°K)	P ₅ (atm)	τ _{ig} (msec)
1293	10.6	.65
1221	9.4	.85
1125	8.1	2.00
1134	8.3	1.62
1152	8.6	1.35
1239	20.1	.22
1287	21.1	.10
1158	17.3	.98
1176	18.0	.58
1293	21.3	.10
1164	17.5	.75
1089	30.6	2.05
1176	36.1	.54
1074	30.1	1.69
1152	34.2	.75
1134	63.3	.44
1050	57.0	1.15
1107	62.6	.75

Table V

Ignition delay data for 70% N₂, 15% CO, 15% N₂O (Fig 17)

T ₅ (°K)	P ₅ (atm)	τ _{ig} (msec)
1236	9.4	.98
1335	10.7	.15
1236	9.4	1.00
1464	10.5	.10
1245	9.4	.85
1260	10.0	.70
1119	30.6	1.17
1212	35.7	.30
1119	30.6	1.38
1104	29.8	1.80
1278	19.7	.10
1275	19.4	.10
1212	17.9	.48
1260	19.4	.12
1173	16.8	1.00
1194	17.3	.65
1275	20.0	.10
1182	68.0	.44
1146	65.3	.87
1098	58.1	1.35
1131	63.1	1.02

Table VI

Ignition delay data for 80% N₂, 10% CO, 10% N₂O (Fig 18)

T ₅ (°K)	P ₅ (atm)	τ _{ig} (msec)
1368	10.3	.15
1269	8.8	1.10
1254	8.6	.60
1245	8.5	1.15
1236	16.7	.90
1221	16.3	1.41
1317	19.0	.12
1245	17.1	.75
1221	32.7	.80
1206	32.4	1.15
1203	31.7	1.35
1227	33.0	.68
1236	50.1	.55
1281	54.3	.15
1221	49.1	.52

Appendix B

Reflected Shock Temperature and Pressure Ratios

The values of T_5/T_1 and P_5/P_1 versus Mach (M) calculated by modifying Craig's equilibrium He/air computer program and used to plot the graphs of Figs 3 through 8 are tabulated in this appendix.

Table VII

T_5/T_1 and P_5/P_1 versus M values for the 60% N_2 , 20% CO, 20% N_2O test gas mixture with helium driver (Figs 3 and 6)

M	T_5/T_1	P_5/P_1
1.185	1.227	2.13
1.217	1.265	2.39
1.249	1.303	2.66
1.281	1.342	2.95
1.313	1.381	3.26
1.501	1.614	5.49
1.795	2.000	10.53
2.061	2.376	16.92
2.306	2.739	24.40
2.534	3.086	32.76
2.749	3.542	42.40
2.953	3.922	52.66
3.150	4.313	63.83
3.340	4.704	75.90
3.526	5.104	88.97
3.708	5.513	103.12
3.813	5.724	107.84
3.971	6.093	120.58
4.175	6.461	133.68
4.274	6.829	147.13
4.419	7.197	160.91
4.561	7.564	174.99
4.699	7.930	189.35
4.835	8.295	203.99
4.967	8.658	218.87
5.097	9.018	233.99
5.225	9.386	249.40
5.350	9.745	264.98
5.472	10.102	280.76
5.593	10.460	296.73
5.711	10.800	312.89
5.829	11.150	329.22

Table VIII

T_5/T_1 and P_5/P_1 versus M values for the 70% N_2 , 15% CO , 15% N_2O test
gas mixture with helium driver (Figs 4 and 7)

M	T_5/T_1	P_5/P_1
1.182	1.227	2.11
1.213	1.265	2.35
1.245	1.304	2.62
1.276	1.343	2.90
1.308	1.382	3.20
1.492	1.616	5.35
1.780	2.006	10.19
2.041	2.386	16.29
2.281	2.753	23.36
2.504	3.108	31.30
2.713	3.577	40.41
2.912	3.957	49.99
3.103	4.340	60.35
3.288	4.729	71.49
3.467	5.126	83.46
3.643	5.522	96.28
3.741	5.715	99.86
3.897	6.087	111.81
4.048	6.459	124.08
4.195	7.189	149.52
4.477	7.555	162.70
4.613	7.921	176.14
4.747	8.284	189.84
4.877	8.646	203.78
5.005	9.006	217.95
5.130	9.363	232.23
5.253	9.716	246.91
5.374	10.075	261.73
5.493	10.420	276.69
5.610	10.770	291.83
5.725	11.110	307.14

Table IX

T_5/T_1 and P_5/P_1 versus M values for the 80% N_2 , 10% CO, 10% N_2O test gas mixture with helium driver (Figs 5 and 8)

M	T_5/T_1	P_5/P_1
1.179	1.227	2.08
1.210	1.266	2.32
1.241	1.305	2.58
1.271	1.343	2.85
1.302	1.383	3.14
1.483	1.619	5.22
1.764	2.012	9.86
2.020	2.397	15.67
2.255	2.771	22.39
2.472	3.133	29.89
2.677	3.614	38.47
2.870	3.992	47.41
3.056	4.371	56.99
3.235	4.753	67.21
3.408	5.140	78.10
3.576	5.532	89.67
3.667	5.702	92.24
3.820	6.071	103.34
3.969	6.441	114.77
4.113	6.810	126.51
4.254	7.179	138.54
4.391	7.548	150.86
4.525	7.909	163.39
4.656	8.272	176.19
4.784	8.632	189.21
4.910	8.990	202.45
5.033	9.345	215.89
5.154	9.696	229.51
5.273	10.040	243.32
5.390	10.390	257.30
5.505	10.720	271.44
5.618	11.070	285.80

Vita

Robert Edward Case was born [REDACTED] the son [REDACTED]. He graduated from high school in [REDACTED] in 1961, attended Wilmington College, Wilmington, Ohio, and then the United States Military Academy, West Point, New York from which he received the degree of Bachelor of Science and a commission in the U.S. Army in 1966. He served in Air Defense Artillery in Europe for two years before attending the Chemical Corps Officer Advanced Course at Fort McClellan, Alabama in 1969. While attending this course, he requested and received a direct transfer to the USAF in October 1969. He was a ballistic missile warning officer in Cheyenne Mountain, Colorado from 1970-1972. He also attended Squadron Officer School at Maxwell AFB, Alabama during that period. In June 1972, he entered the Graduate Astronautical Engineering Program at the Air Force Institute of Technology at Wright-Patterson AFB, Ohio.

Permanent address: [REDACTED]

This thesis was typed by Mrs. Imogene J. Hoffer.